

Article

Hydrochemical Characterization and Quality Assessment of Groundwater in the Southern Plain of Hebei Province, China

Longqiang Zhang ^{1,*}, Donglin Dong ^{1,*}, Situ Lv ¹, Jialun Zhang ¹, Maohua Yan ², Guilei Han ³ and Huizhe Li ¹

¹ College of Geoscience and Surveying Engineering, China University of Mining and Technology (Beijing), Beijing 100083, China; lvsitu@163.com (S.L.); zjl_cumtb@163.com (J.Z.); lihuizhe666@163.com (H.L.)

² China Institute of Geological Environment Monitoring, Beijing 100081, China; yanmaohua@mail.cgs.gov.cn

³ North China Nonferrous Engineering Investigation Institute Co., Ltd., Shijiazhuang 050021, China; hanguilei517@163.com

* Correspondence: zlqcumtb@163.com (L.Z.); ddl9266@163.com (D.D.)

Abstract: The purpose of this research was to understand the hydrogeochemical characteristics and assess the quality of phreatic and confined groundwater in southern Hebei Province. A total of 107 groundwater samples were collected, representing different aquifer conditions over the study area. Multivariate statistical analysis, hydrochemical maps, ionic ratio coefficients, geographic information system (GIS) and geochemical simulation were comprehensively and systematically used to reveal the hydrochemical characteristics of groundwater and its controlling mechanism. The results revealed that both phreatic (pH = 7.02–9.08) and confined groundwater (pH = 7.00–10.60) were slightly alkaline. The hydrochemical types were mainly present as the HCO₃-Ca-Mg type in the western premontane area and mixed Ca-Mg-SO₄-Cl and Na-Cl-SO₄ types in the eastern plains. The hydrochemical composition was dominated by water–rock interactions of natural processes, including silicate weathering, dissolution of sulfate minerals (gypsum, anhydrite), and cation-exchange adsorption. Anthropogenic activities were the main factor causing NO₃⁻ content in some groundwater samples to exceed the geochemical baseline. The hydrogeochemistry of groundwater in different aquifers was significantly varied. The average contents of TH, TDS, Na⁺, Ca²⁺, Mg²⁺, Cl⁻ and SO₄²⁻ in phreatic aquifers were significantly higher than those in confined aquifers. The Entropy Weighted Water Quality Index (EWQI) results revealed that 17.78% of phreatic and 50% of confined water samples were meeting the purpose of drinking water. The groundwater samples with EWQI values exceeding 100 were mainly situated in the Handan urban area and the eastern region of Xingtai City, which should be avoided for direct utilization and needs to be improved through protection and management measures, to enhance the quality of groundwater. Correlation analysis showed that groundwater quality was significantly dominated by TH, TDS, Na⁺, Mg²⁺, Cl⁻ and SO₄²⁻ concentrations.

Keywords: hydrochemistry; water–rock interaction; groundwater quality; EWQI; factor analysis



Citation: Zhang, L.; Dong, D.; Lv, S.; Zhang, J.; Yan, M.; Han, G.; Li, H. Hydrochemical Characterization and Quality Assessment of Groundwater in the Southern Plain of Hebei Province, China. *Water* **2023**, *15*, 3791. <https://doi.org/10.3390/w15213791>

Academic Editors: C. Radu Gogu and Oana Luca

Received: 6 August 2023

Revised: 11 September 2023

Accepted: 21 September 2023

Published: 29 October 2023



Copyright: © 2023 by the authors. Licensee MDPI, Basel, Switzerland. This article is an open access article distributed under the terms and conditions of the Creative Commons Attribution (CC BY) license (<https://creativecommons.org/licenses/by/4.0/>).

1. Introduction

Groundwater is a fundamental resource that is essential to ensuring sustainable socioeconomic development [1,2]. Groundwater resources account for about 99% of all liquid freshwater resources in the world, and more than 50% of the world's residents' domestic water comes from groundwater, and about 25% of agricultural irrigation water also comes from groundwater [3,4]. Therefore, groundwater resources play an essential role in ensuring human survival, sustaining industrial and agricultural development and controlling the ecological balance [5–7]. However, explosive global population growth and accelerated industrialization have led to dramatic decrease of global groundwater resources. Many regions in the world are facing multiple pressures on groundwater resources and groundwater environmental problems, such as groundwater resource shortage, groundwater pollution and frequent occurrence of extreme hydrogeological conditions [8–10]. When groundwater resources in some areas, especially in underdeveloped areas, are completely depleted and there are no

other sources of water to utilize, the survival of the local people will be unsustainable, and they can only leave their homes and become “water refugees” [11,12]. Once such a situation occurs, it will threaten the security and stability of the world situation to a great extent. Therefore, the protection of groundwater resources is related to the common well-being of natural ecosystems and human beings, and it is urgent.

Hydrogeochemical research is the theoretical basis for realizing the rational utilization of groundwater resources and the effective protection of the groundwater environment, which can reveal the influence and relationship of various hydrogeochemical effects and anthropogenic activities on various geological phenomena during the formation of groundwater [13,14]. Further understanding the hydrochemical characteristics and quality status of groundwater resources is essential to help people select suitable water sources, formulate scientific water management policies and prevent groundwater pollution [15,16]. The hydrogeochemical characteristics can reflect the evolutionary patterns and control mechanisms of groundwater, which are divided into natural processes and anthropogenic activities [17]. Natural processes mainly include dissolution of carbonates, sulfates, silicates, halite and cation exchange [18–20]. To comprehensively grasp and understand the hydrochemical composition and control mechanisms of groundwater, many scholars have used multivariate statistical analysis methods to classify hydrogeochemical parameters and effectively extract the major components that determine the hydrogeochemical composition [21,22]. Major ion ratio coefficients can be used to conclude the physical similarity of groundwater chemical components and the hydrogeochemical processes undergone. A piper trilinear diagram is able to reveal the hydrogeochemical types, but cannot present the distribution and evolution of the hydrogeochemical classification on the spatial scale. Hydrogeochemical models are able to simulate the saturation indices of specific minerals but are also deficient in presenting spatial characteristics. The geographic information system (GIS) has been widely used in the research of various fields with its powerful graphics and visualization functions [23]. Therefore, it is reasonable and feasible to study hydrogeochemical characteristics and quality assessments of groundwater by combining GIS and a hydrochemical graphic method.

The southern plains of Hebei Province are extremely scarce in water resources, and urban industrial and agricultural production, living, and ecological water rely on groundwater resources to a large extent [24,25]. In recent years, under the double pressure of severe water resource shortage and sustainable economic and social development, a series of geological and environmental problems such as the decline of groundwater level, the drying of aquifers and the deterioration of water quality have appeared which are due to the long-term overexploitation of groundwater. The excessive consumption of regional groundwater resources and environmental pollution have caused great pressure on the local ecological environment [26–29]. Many scholars have previously performed a lot of research on groundwater in the Hebei Plain, mainly focused on the amount of groundwater resources [30,31], but relatively little research on the environmental aspects of groundwater in the region. In particular, the hydrogeochemical characteristics and spatial distribution patterns of water quality of shallow phreatic and deep karst confined groundwater in the southern Hebei Province needs to be urgently clarified. Therefore, to meet the needs of the construction of a regional water conservation function area and ecological environment support area, and to guarantee the safety of groundwater resources and the ecological environment, it is especially necessary to carry out investigations and research on the groundwater environment in the southern Hebei Province.

Groundwater samples from 45 phreatic monitoring wells and 62 pressurized water monitoring wells were investigated to gain insight into the hydrochemical characteristics and water quality of different aquifers in the southern region of the Hebei Province. The present research aims to (1) systematically reveal the hydrochemical characteristics and control mechanisms of groundwater from different aquifers in southern Hebei Province by using a variety of methods; (2) to simulate and deduce the hydrogeochemical processes and evolution of groundwater; (3) use EWQI and GIS to spatially classify groundwater

quality and evaluate its feasibility for drinking water; and (4) to reveal the indicators that mainly affect the quality of groundwater and to propose corresponding protection and countermeasures. The results of this study will fill the lack of research on the groundwater environment in the southern Hebei Province, and provide a scientific basis for regional groundwater environmental protection and pollution prevention and remediation. The main innovations of this study were as follows:

- (1) In this paper, ArcGIS spatial analysis is combined with the hydrochemical graphic method to systematically reveal the spatial distribution characteristics of groundwater hydrochemistry, which effectively makes up for the deficiency in the hydrochemical graphic method in studying spatial scale.
- (2) A clustering analysis was introduced to reveal the source similarity of ions and its influence relationship.
- (3) The correlation analysis and entropy weight water quality index were combined to identify and optimize the main impact indicators of water quality, and further reduce the cost of water quality monitoring.

2. Study Area

The study area is bounded by the Taihang Mountains in the west and the North China Plain in the east and extends between $36^{\circ}03'–37^{\circ}47'$ N latitude and $113^{\circ}30'–115^{\circ}50'$ E longitude (Figure 1). The terrain is arranged in a ladder form from the west to the east mountains, hills and plains [32]. The study area has the warm-temperate semi-humid and semi-arid continental monsoon climate, with an average annual precipitation of 566.8 mm and an average annual evaporation of 1702.5 mm [33]. The eastern plain is rich in various agricultural products and cash crops, while the western plain is rich in mineral resources, providing diversified resources for local economic development.

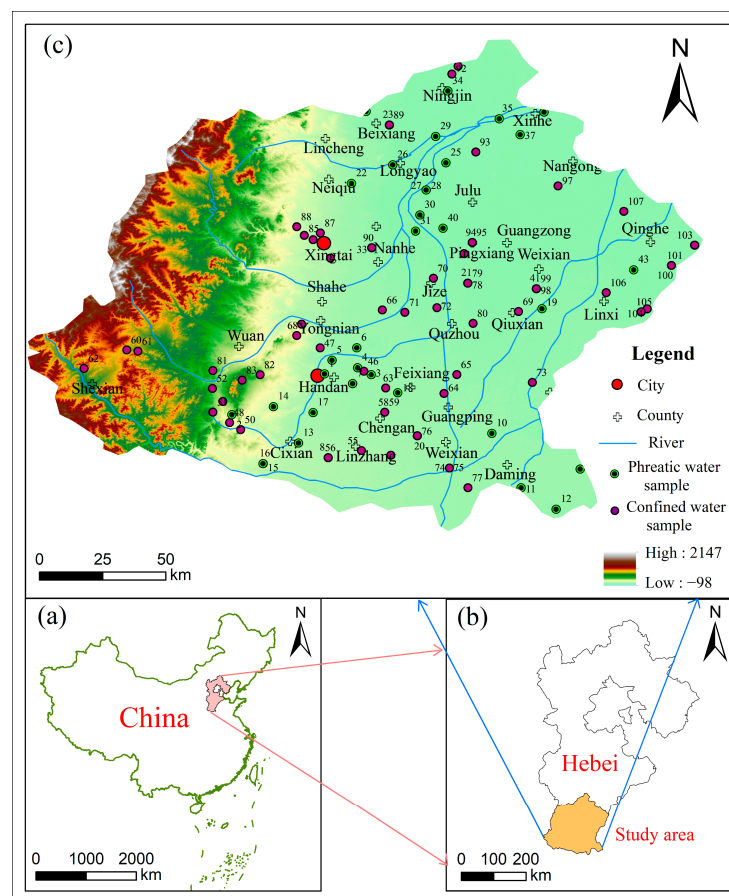


Figure 1. (a) Geographical location map of Hebei Province, (b) Location map of the study area in Hebei Province, (c) Map of sampling locations.

The spatial distribution of lithology in the study area from west to east is characterized by quartz sandstone, gneiss, limestone and quaternary loose beds. Groundwater types mainly include loose rock pore water, limestone karst water and metamorphic rock fissure water. The flow direction of pore water in the quaternary loose rock type is generally consistent with the topography. Karst groundwater is stored in the carbonate rock strata of the Lower Paleozoic and is mainly distributed in the pre-mountain plains around Xingtai, Shahe, Neiqiu and Lincheng. Metamorphic rocks and magmatic fissure water are widely exposed in the mountainous areas, with short flow and shallow burial without obvious recharge, runoff and discharge areas.

3. Materials and Methods

3.1. Sample Collection and Analysis

Groundwater samples were collected in August 2021 from 107 wells in the southern Hebei Province, including 45 quaternary pore-phreatic and 62 karst confined groundwater samples (Figure 1c). To ensure the freshness of the water samples collected, water was pumped for 15 min before sampling. The water samples were filtered through a 0.45 µm pore size microporous membrane to remove suspended solids, and then stored in two 100 mL polyethylene plastic bottles. The one bottle of water sample for cation testing was acidified to pH < 2 with high-purity nitric acid, while the other bottle of water sample for anion testing did not require the addition of other reagents. All groundwater samples were sealed in a dark box at 4 °C and sent to the Hebei Environmental Monitoring Institute for ion testing within 48 h. Temperature (T), pH and dissolved oxygen (DO) were measured in situ using a high precision, portable, multi-parameter water quality meter (Multi 350i/SET, Munich, Germany) produced by WTW. For the indoor analysis, the main cation components were analyzed by an inductively coupled plasma atomic emission spectrometer (Agilent 5100 ICP-OES, Santa Clara, CA, USA). Anionic components were measured by ion chromatography (Thermo ICS-1100, Stoney Creek, CA, USA). The anion and cation balances for all samples were within 5% (1). Data were processed and analyzed using SPSS version 2022; groundwater chemistry was mapped using Origin 2021; and hydrogeochemical simulations were carried out using PHREEQC2.11.

$$\%CBE = \frac{TZ^+ - TZ^-}{TZ^+ + TZ^-} \times 100\% \quad (1)$$

In Formula (1), $TZ^+ = Na^+ + K^+ + Mg^{2+} + Ca^{2+}$, $TZ^- = HCO_3^- + SO_4^{2-} + NO_3^- + Cl^- + F^-$.

3.2. Hydrogeochemical Modeling

PHREEQC2.11 is computer software for calculating hydrogeochemical reactions based on the ionic conjugate water model [34]. The software is widely used to calculate mineral saturation indices (SI), to infer the possible dissolution or precipitation of minerals in different hydrogeochemical pathways and to reveal the possible evolution of groundwater chemistry. Saturation index is a thermodynamic index that qualitatively represents the tendency of various minerals to precipitate and dissolve in groundwater. The calculation formula is as follows:

$$SI = \lg \frac{IAP}{K} \quad (2)$$

In Formula (2), IAP is the ionic activity product and K is the equilibrium constant. If $SI < 0$, the solution is unsaturated. $SI = 0$ when the solution is saturated; $SI > 0$ means that the solution is supersaturated and precipitation is possible.

3.3. Entropy Weighted Water Quality Index (EWQI)

Entropy weighted water quality index (EWQI) is the evaluation model developed based on the information entropy theory to completely reflect the groundwater quality information through the real weights of several physicochemical parameters [35]. It is widely used in the quantitative assessment of groundwater quality by virtue of its simplicity and accuracy and can solve the problems existing in other groundwater quality evaluation techniques [36]. The main calculation process is as follows:

Step 1: Firstly, the characteristic matrix X is constructed.

$$X = \begin{pmatrix} x_{11} & x_{12} & \dots & x_{1n} \\ x_{21} & x_{22} & \dots & x_{2n} \\ \vdots & \vdots & x_{ij} & \vdots \\ x_{m1} & x_{m2} & \dots & x_{mn} \end{pmatrix} \quad (3)$$

where, m is the number of groundwater samples collected, and the value is $i = 1, 2, \dots, m$; n indicates the selected quality parameter, the value is $j = 1, 2, \dots, n$; x_{ij} is the jth parameter of the ith sample.

Step 2: Standardized data.

$$y_{ij} = \frac{x_{ij} - (x_j)_{\min}}{(x_j)_{\max} - (x_j)_{\min}} \in (0, 1) \quad (4)$$

where, $(x_j)_{\min}$ and $(x_j)_{\max}$ are the min and max values of the jth hydrochemical index in the initial matrix, respectively.

Step 3: Determine the weight.

$$P_{ij} = \frac{y_{ij}}{\sum_{i=1}^m (y_{ij})} \in (0, 1) \quad (5)$$

$$e_j = -\frac{1}{\ln(m)} \sum_{i=1}^m (P_{ij} \ln P_{ij}) \quad (6)$$

$$w_j = \frac{1 - e_j}{\sum_{j=1}^n 1 - e_j} \in (0, 1) \quad (7)$$

where, e_j is the information entropy of hydrochemical parameter index, and w_j is the entropy weight of the hydrochemical indicator.

Step 4: Determine the quantitative standard of classification.

$$q_{ij} = \begin{cases} (c_j/s_j) \times 100 \\ |(c_{ipH} - 7)/(8.5 - 7) \times 100| \end{cases} \quad (8)$$

where, c_j is the content of each physicochemical parameter in the groundwater sample, and s_j is the permissible limit of the physicochemical parameter specified in the drinking water standard.

Step 5: Calculating EWQI.

$$EWQI = \sum_{j=1}^n w_j q_j \quad (9)$$

where, q_j is the quality rank corresponding to each groundwater sample.

3.4. Research Content and Technical Route

The program and technical route of the study was shown in Figure 2. The detailed steps of the program were as follows:

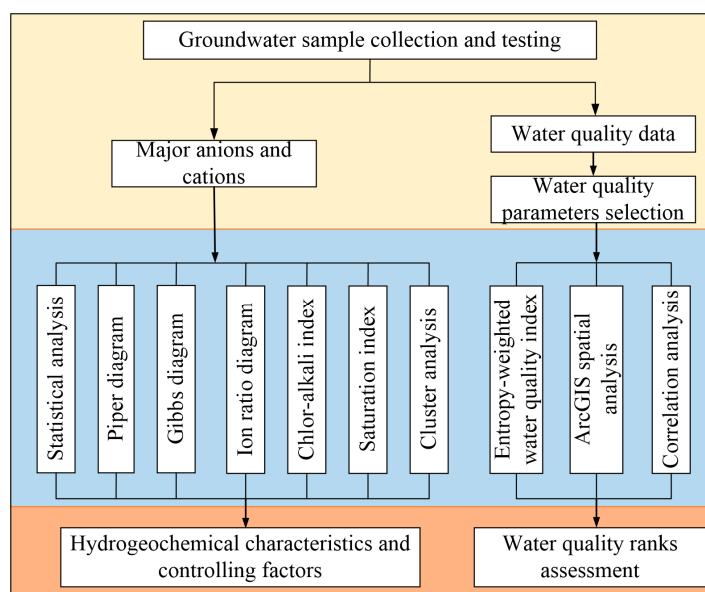


Figure 2. Technology roadmap.

Step 1: Data collection and selection.

The major anions (SO_4^{2-} , HCO_3^- , Cl^-), cations (Na^+ , Ca^{2+} , Mg^{2+} , K^+) and physical parameters (pH, TH, TDS) of 107 collected groundwater samples were measured, and the water quality evaluation index parameters were selected.

Step 2: Hydrogeochemical characteristics and control mechanism.

Based on the hydrochemical parameters, the characteristics of the major anions and cations were analyzed. The chemical types and spatial distribution of phreatic and confined groundwater were revealed by ArcGIS and piper maps. Multiple methods including Gibbs diagrams, ionic ratios, chlor-alkali indices, saturation indices, and cluster analyses were comprehensively applied to elucidate the hydrochemical characterization of groundwater and its controlling mechanisms.

Step 3: Groundwater quality assessment.

The entropy-variable weighted water quality index and ArcGIS spatial analysis were used to spatially classify groundwater quality ranks, and correlation analysis was used to reveal the main index parameters affecting water quality.

4. Results and Discussion

4.1. Hydrochemical Characteristics

Hydrochemical characteristics can preserve and invert the information of groundwater affected by regional geological structure, hydrodynamic conditions and human activities. In this study, several statistics of 12 physicochemical parameters in phreatic and confined groundwater were analyzed by descriptive statistics, and the results are presented in Table 1. Groundwater of phreatic and confined aquifers in the southern Hebei Province presented as slightly alkaline, with average pH values of 7.45 and 8.02, respectively. The ranges of TH and TDS in the phreatic groundwater were 268~2646.00 mg/L and 342~5843.00 mg/L, and those in the confined groundwater were 11.60~2337.00 mg/L and 154.00~5052.00 mg/L. The average concentrations of TH and TDS in the groundwater of the phreatic aquifer in the study area were significantly higher than those in confined aquifers, and both of them were higher than the limit values permitted by the drinking water standards (Table 1). The TH and TDS concentrations exceeding the recommended limit values were mainly concentrated in the east-central and southeast of the study area, showing an evolutionary pattern of gradually increasing concentrations from the western mountainous areas to the eastern plain (Figure 3).

Table 1. Statistical analysis of physicochemical parameters in phreatic and confined groundwater samples.

Parameters	Guideline	Phreatic Groundwater					Confined Groundwater				
		Min.	Max.	Ave.	SD	CV (%)	Min.	Max.	Ave.	SD	CV (%)
pH	6.5–8.5 *	7.02	9.08	7.45	0.39	5.31	7.00	10.60	8.02	0.87	10.87
TH	450 *	268	2646.00	825.10	624.72	75.71	11.60	2337.00	478.20	509.26	106.49
TDS	1000 *	342	5843.00	1772.22	1354.46	76.42	154.00	5052.00	1062.35	1080.78	101.73
Na ⁺	200 *	2.69	1127.00	318.72	302.14	94.79	9.35	996.00	207.97	233.43	101.73
K ⁺		0.34	4.46	1.53	0.97	63.69	0.36	8.41	1.38	1.06	77.40
Ca ²⁺	75 **	4.87	480.00	131.39	98.58	75.03	0.98	288.00	78.33	70.02	89.39
Mg ²⁺	50 **	1.29	490.00	120.71	115.30	95.51	1.90	398.00	68.97	92.92	134.73
Cl ⁻	250 *	4.20	1672.00	328.06	355.92	105.98	8.50	1439.00	223.30	318.83	142.78
SO ₄ ²⁻	250 *	3.66	2114.00	594.26	588.77	129.07	8.65	2192.00	329.48	480.54	145.84
HCO ₃ ⁻		25.00	1321.00	485.51	248.94	51.27	16.00	771.00	276.77	150.17	54.25
NO ₃ ⁻	50 **	0.29	145.00	9.85	22.72	230.65	0.15	35.9	4.08	6.30	194.39
F ⁻	1.0 *	0.20	2.99	0.83	0.58	70.44	0.16	3.10	0.91	0.75	113.40

Note: * Chinese Guideline [37]; ** WHO Guideline [38].

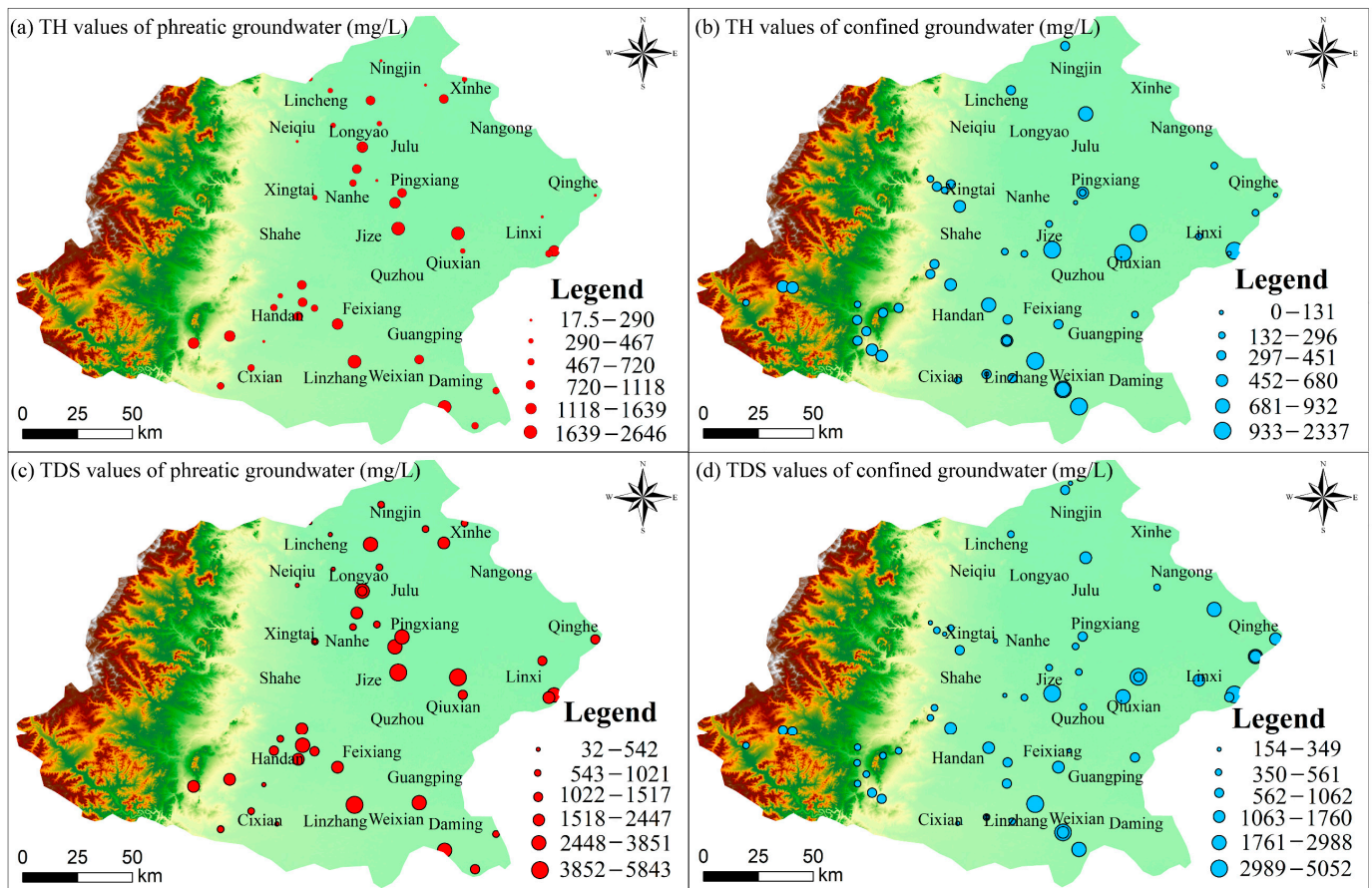


Figure 3. Spatial patterns of TH and TDS in phreatic and confined groundwater.

The order of concentration for conventional anions and cations in groundwater from two different aquifers was listed as $SO_4^{2-} > HCO_3^- > Cl^- > NO_3^- > F^-$ and $Na^+ > Ca^{2+} > Mg^{2+} > K^+$. Except for F^- , the concentrations of other ions in phreatic aquifer were significantly higher than those in confined aquifer. It was mainly due to the high pH in the confined aquifer, and the alkaline environment was more favorable for the adsorption and enrichment of F^- . The box plots of major anion and cation concentrations in groundwater from phreatic and confined aquifers are presented in Figures 4 and 5. It can be seen that

the concentration of each ion varies significantly, especially Na^+ , Mg^{2+} , Cl^- , SO_4^{2-} , and NO_3^- which have larger SD and CV values than the other ions. According to the mean and median values, the concentrations of Na^+ , Ca^{2+} , Mg^{2+} , SO_4^{2-} , HCO_3^- , and Cl^- in phreatic and confined groundwater all exceeded the limit values for drinking purposes, indicating that the groundwater in the south of Hebei Province was highly mineralized and the water quality needed to be further improved.

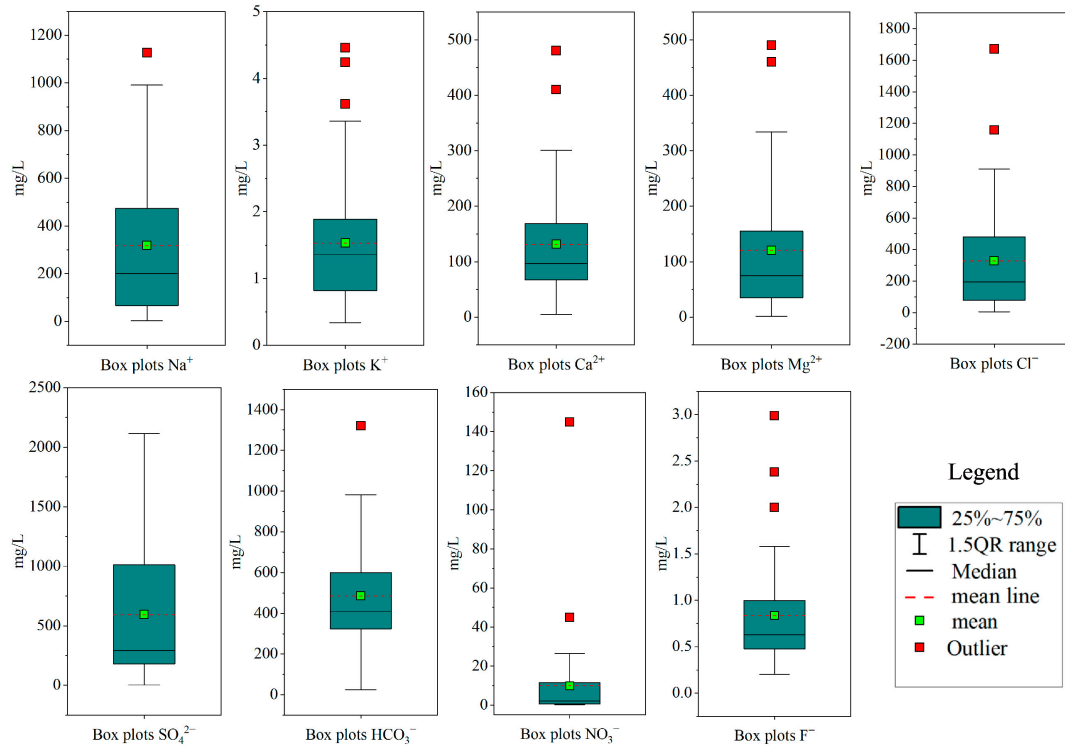


Figure 4. Box plots of major ions in phreatic groundwater.

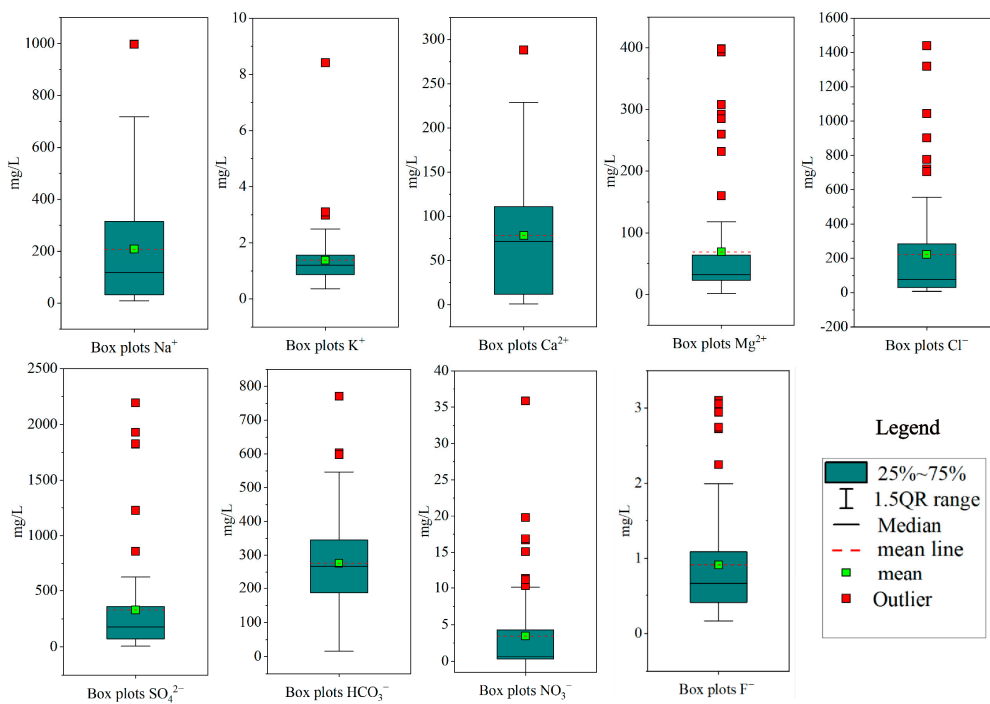


Figure 5. Box plots of major ions in confined groundwater.

The hydrochemical type of groundwater is a concentrated reflection of the chemical composition of groundwater, and it is also an important part of the study of the hydro-geochemical characteristics of groundwater. The piper diagram was an essential method used to identify the hydrogeochemical phases of groundwater [39]. In this study, a piper diagram of phreatic and confined groundwater was plotted using Aqua Chem version 2014 software (Figure 6). In all phreatic groundwaters, Ca-Mg-HCO₃, Na-Cl-SO₄, Na-HCO₃-Cl, Ca-Mg-SO₄-Cl and Ca-Mg-SO₄ types of water accounted for 28.88%, 22.22%, 6.67%, 26.66% and 13.33%, respectively. Confined groundwaters were mainly classified into three types, including Ca-Mg-HCO₃, Ca-Mg-SO₄-Cl and Na-Cl-SO₄ types. Along the path of groundwater runoff, the hydrochemical type gradually evolved from fresh HCO₃-Ca-Mg water to brackish Cl-SO₄-Na water. In general, most groundwater hydrochemical types in the southern plain of the Hebei Province were fresh HCO₃-Ca and brackish Ca-Mg-Cl mixed types. Compared with phreatic groundwater, confined groundwater displayed fresher characteristics.

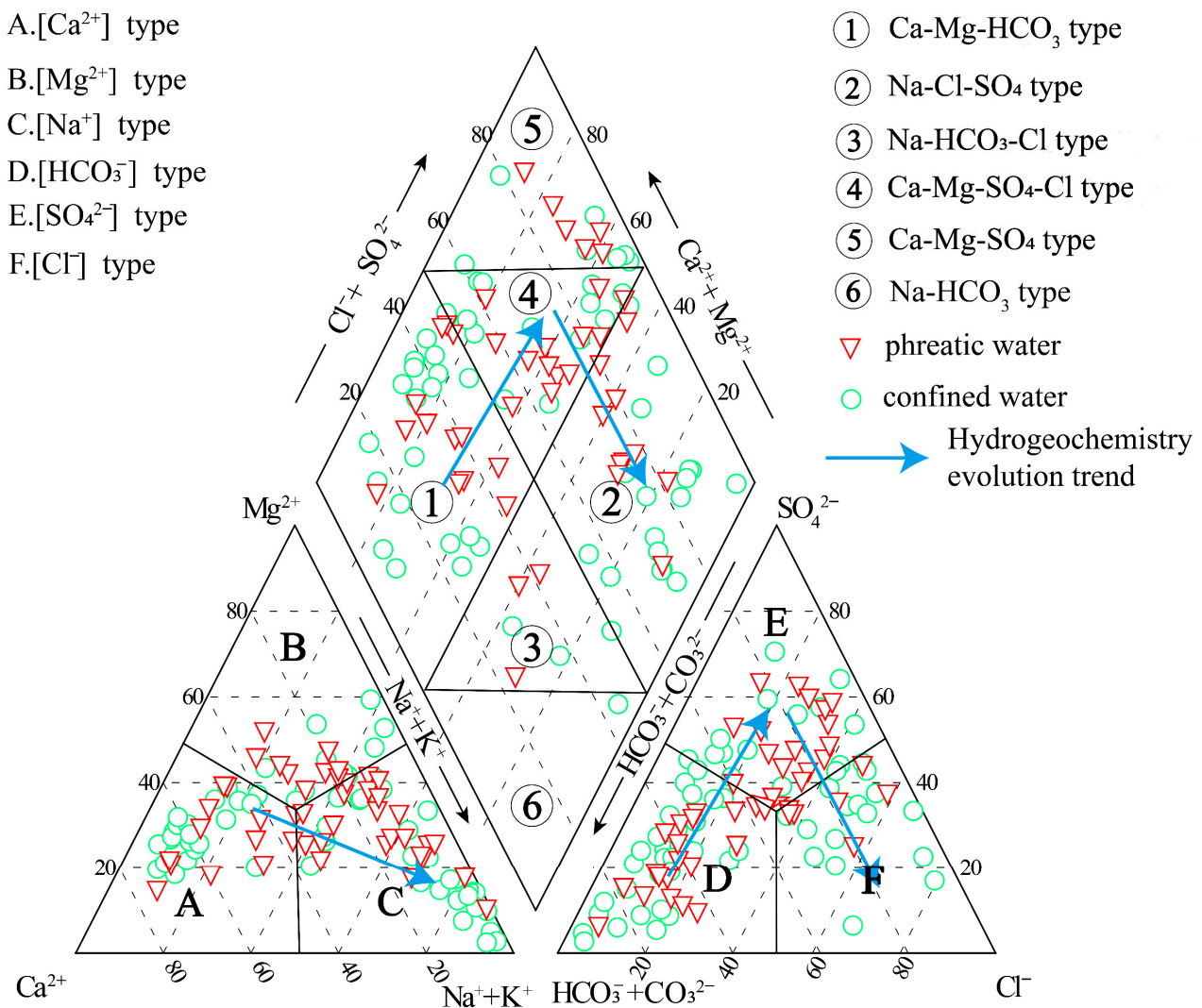


Figure 6. Piper diagram for phreatic and confined groundwaters.

Understanding the spatial distribution pattern of groundwater hydrochemical types not only helps to recognize the hydrogeochemical characteristics of regional groundwater, but also contributes to the in-depth study of the circulation characteristics and hydrodynamic characteristics of regional groundwater. To further study the spatial distribution characteristics and evolutionary patterns of groundwater types, geospatial analysis was introduced to spatially classify the hydrogeochemical types of phreatic and confined

groundwater (Figure 7). Figure 7 revealed that the hydrochemical type of phreatic groundwater was fresh $\text{HCO}_3\text{-Ca-Mg}$ type water in the northwest and southwest of the study area, $\text{Ca-Mg-SO}_4\text{-Cl}$ type water in the central region, and Na-Cl-SO_4 type water in the eastern margin. Compared to the western mountainous areas, the intensity of groundwater extraction in the central and eastern plains is high, the water table gradually decreases, the thickness of the gas-saturated zone increases, and the natural chemical balance in the groundwater aquifers is disrupted, resulting in increased concentrations of Cl^- , SO_4^{2-} and Na^+ . For confined aquifers, fresh Ca-Mg-HCO_3 type water is dominant in the western piedmont area, while Na-Cl-SO_4 and $\text{Ca-Mg-SO}_4\text{-Cl}$ types of water are dominant in the central and eastern plain areas. Compared to phreatic groundwater, confined groundwater presents fresher characteristics in the western premontane area, while it shows more brackish characteristics in the central and eastern plains.

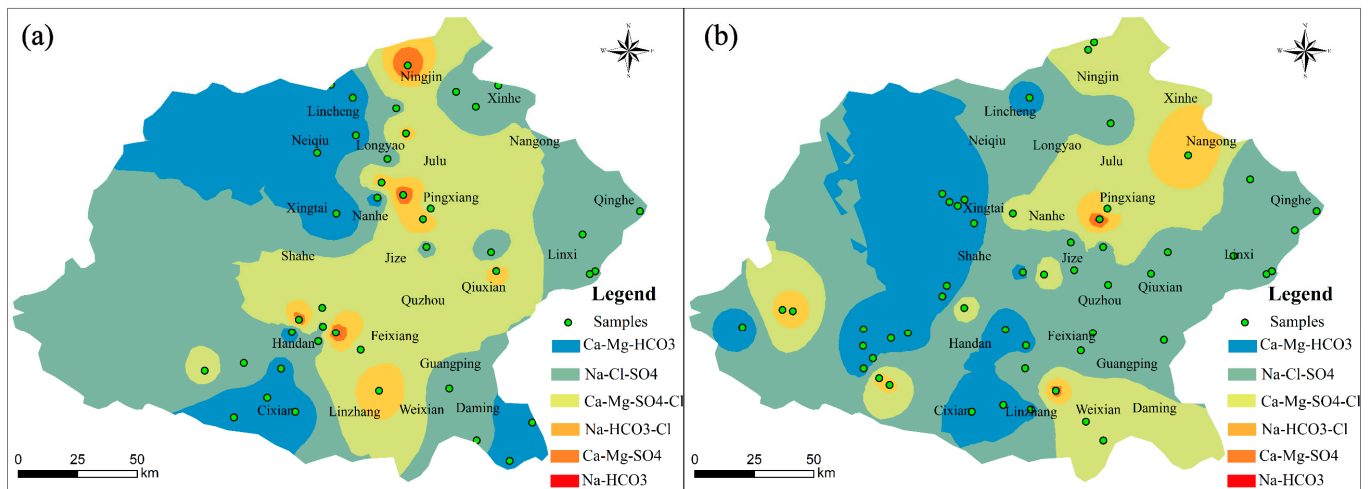


Figure 7. Spatial map of hydrochemical types for (a) phreatic groundwater and (b) confined groundwater.

4.2. Mechanism Controlling Groundwater Hydrochemistry

4.2.1. Natural Factors Affecting Groundwater Hydrochemistry

The water chemistry in groundwater can reflect the characteristics of the groundwater flow system and is generally controlled by different factors. According to R.J. Gibbs, the various effects on the hydrogeochemical composition are mainly divided into three mechanisms: concentration crystallization, atmospheric precipitation, and rock weathering and dissolution [40]. The Gibbs plot can clearly represent the dominant factors of the chemical composition of groundwater. Figure 8a,b revealed that most samples were mapped in the region of rock dissolution and only a few phreatic samples fell in the region of evapotranspiration, suggesting that rock dissolution is the dominant factor in the chemical composition of groundwater in phreatic and confined aquifers. Evaporation mainly affected a small amount of shallowly buried phreatic water samples in the east. Notably, the $\text{Na}^+ / (\text{Na}^+ + \text{Ca}^{2+})$ ratios of the water samples were scattered in different intervals from 0 to 1, suggesting that cation exchange processes existed in the two aquifers at different depths. The ion three-terminal diagram can reveal the type of water–rock interaction that occurs during the evolution of groundwater chemistry [41]. Most of the water samples were plotted in the silicate-dominated region, and only a few water samples from the deep, confined aquifer fell near the carbonate region (Figure 8c,d), suggesting that the water–rock interaction in the two aquifers is mainly dominated by silicate dissolution, and the dissolution of carbonate has a potential impact mainly on the deep confined aquifer.

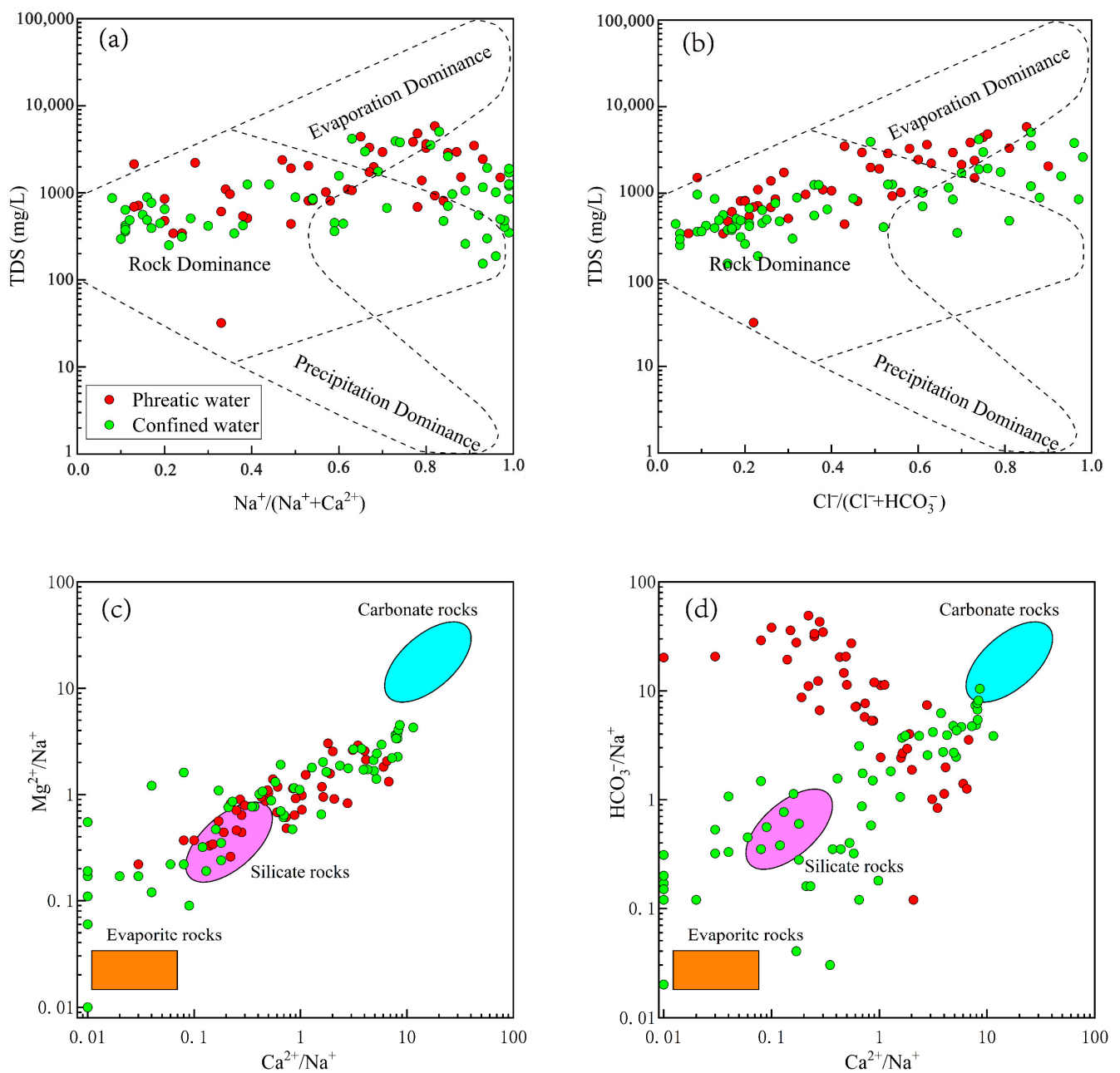
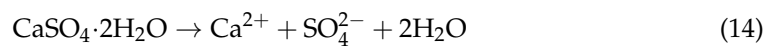
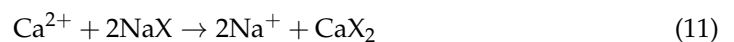


Figure 8. The Gibbs diagram revealing the hydrochemical mechanisms controlling phreatic and confined groundwater, (a) TDS versus $\text{Na}^+ / (\text{Na}^+ + \text{Ca}^{2+})$, (b) TDS versus $\text{Cl}^- / (\text{Cl}^- + \text{HCO}_3^-)$, and scatter plots of molar ratios (c) $(\text{Mg}^{2+} / \text{Na}^+)$ versus $(\text{Ca}^{2+} / \text{Na}^+)$, (d) $(\text{HCO}_3^- / \text{Na}^+)$ versus $(\text{Ca}^{2+} / \text{Na}^+)$.

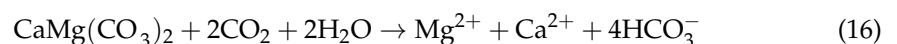
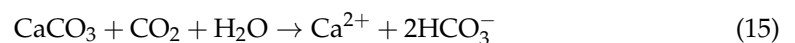
Ion ratios are useful to improve understanding in depth of hydrogeochemical processes in groundwater [42]. Most of the water samples were observed below the 1:1 line (Figure 9a), indicating that Na^+ concentrations in both aquifers are excessive relative to the Cl^- content, besides, halite dissolution (10), ion-exchange (11) and silicate-dissolution (12) processes are also material sources of Na^+ in groundwater. This also confirmed the conclusions in Figure 7 above. The molar ratios of Ca^{2+} and SO_4^{2-} (Figure 9b) revealed that most groundwater samples plotted along a 1:1 line, implying SO_4^{2-} and Ca^{2+} in phreatic and confined groundwaters are probably sourced from the dissolution of sulfate minerals (gypsum (13) and anhydrite (14)). Some phreatic groundwater samples were observed above the 1:1 line (Figure 9b), suggesting that there may be other sources of SO_4^{2-} in the phreatic aquifer besides dissolved sulfate minerals [43]. In addition, the depletion

of Ca^{2+} in groundwater by cation exchange also leads to an excess of SO_4^{2-} relative to Ca^{2+} in aquifers. Therefore, it is concluded that the dissolution of gypsum and anhydrite significantly contributes to Ca^{2+} and SO_4^{2-} in phreatic and confined groundwater within the study area, and the dissolution of other sulphate minerals and cation exchange are also potentially involved in the hydrogeochemical mechanisms of phreatic groundwater. Therefore, the contents of Ca^{2+} and SO_4^{2-} in phreatic and confined groundwater in the southern Hebei Province were mainly affected by the dissolution of sulfate minerals, and cation-exchange interactions also potentially contributed to the hydrogeochemistry of the phreatic groundwater.



The ratio coefficient of $\text{Mg}^{2+}/\text{Ca}^{2+}$ can reveal and distinguish the contribution of dissolution from different carbonate and silicate minerals to the chemical composition of groundwater [44]. When the $\text{Mg}^{2+}/\text{Ca}^{2+}$ ratio is higher than 1, equal to 1 and less than 0.5, respectively, it indicates that the ions originate from the dissolution of silicates, calcite (15), and gypsum (16), respectively. In this study, the phreatic water samples mainly fell above 1:1 and near the 1:2 line, indicating that the chemical composition of phreatic groundwater was mainly derived from the dissolution of sulfate and silicate minerals. Most of the karst confined groundwater samples were distributed below 1:1 (Figure 9c), indicating that the chemical composition of confined groundwater was mainly from the dissolution of calcite and silicate minerals.

The $(\text{Ca}^{2+} + \text{Mg}^{2+})$ and $(\text{HCO}_3^- + \text{SO}_4^{2-})$ bivariate maps can effectively distinguish the potential contribution of ion exchange interactions, carbonate and sulfate dissolution to the hydrochemical composition of groundwater. The milliequivalent ratio equal to 1 indicates that sulphate and carbonate dissolution is the dominant process, and the ratio greater than 1 or less than 1 indicates cation-exchange processes or reverse cation-exchange processes. Most of phreatic and karst confined water samples were observed to be distributed along the 1:1 line, indicating a dissolution process of sulfate and carbonate minerals (Figure 9d). However, some phreatic and confined groundwater samples were plotted above the 1:1 line, suggesting that cation exchange leads to excessive concentrations of HCO_3^- and SO_4^{2-} in groundwater relative to Ca^{2+} and Mg^{2+} .



$(\text{Na}^+ + \text{K}^+ - \text{Cl}^-)/[(\text{Ca}^{2+} + \text{Mg}^{2+}) - (\text{HCO}_3^- + \text{SO}_4^{2-})]$ can be used to analyze the effect of ion exchange on groundwater [45]. From Figure 9a, it was known that the distributions of water samples all fell in or close to the—(1:1) straight line, and the groundwaters of phreatic and confined aquifers in the southern Hebei Province were all affected by ion-exchange action. Confined groundwater samples were mainly concentrated near the origin of coordinates, while some phreatic water samples were far away from the origin, indicating that ion exchange interaction in the phreatic aquifer was more intense, resulting in the elevation of the Na^+ concentration. The chlor-alkali index is an effective examination

of ion exchange in groundwater [46]. When CAI-I and CAI-II are both negative (17,18), it means that Ca^{2+} or Mg^{2+} replaces Na^+ or K^+ in aqueous media in groundwater, while when CAI-I and CAI-II are positive, there is reverse cation exchange. Figure 10b revealed that CAI-I and CAI-II of 80% of the phreatic and 72.58% of the confined groundwater samples were distributed in the third quadrant, indicating that both cation exchange and reverse cation exchange processes are present in phreatic and confined groundwater systems and cation exchange is the dominant process.

$$\text{CAI - I} = \frac{\text{Cl}^- - (\text{Na}^+ + \text{K}^+)}{\text{Cl}^-} \tag{17}$$

$$\text{CAI - II} = \frac{\text{Cl}^- - (\text{Na}^+ + \text{K}^+)}{\text{HCO}_3^- + \text{SO}_4^{2-} + \text{CO}_3^{2-} + \text{NO}_3^-} \tag{18}$$

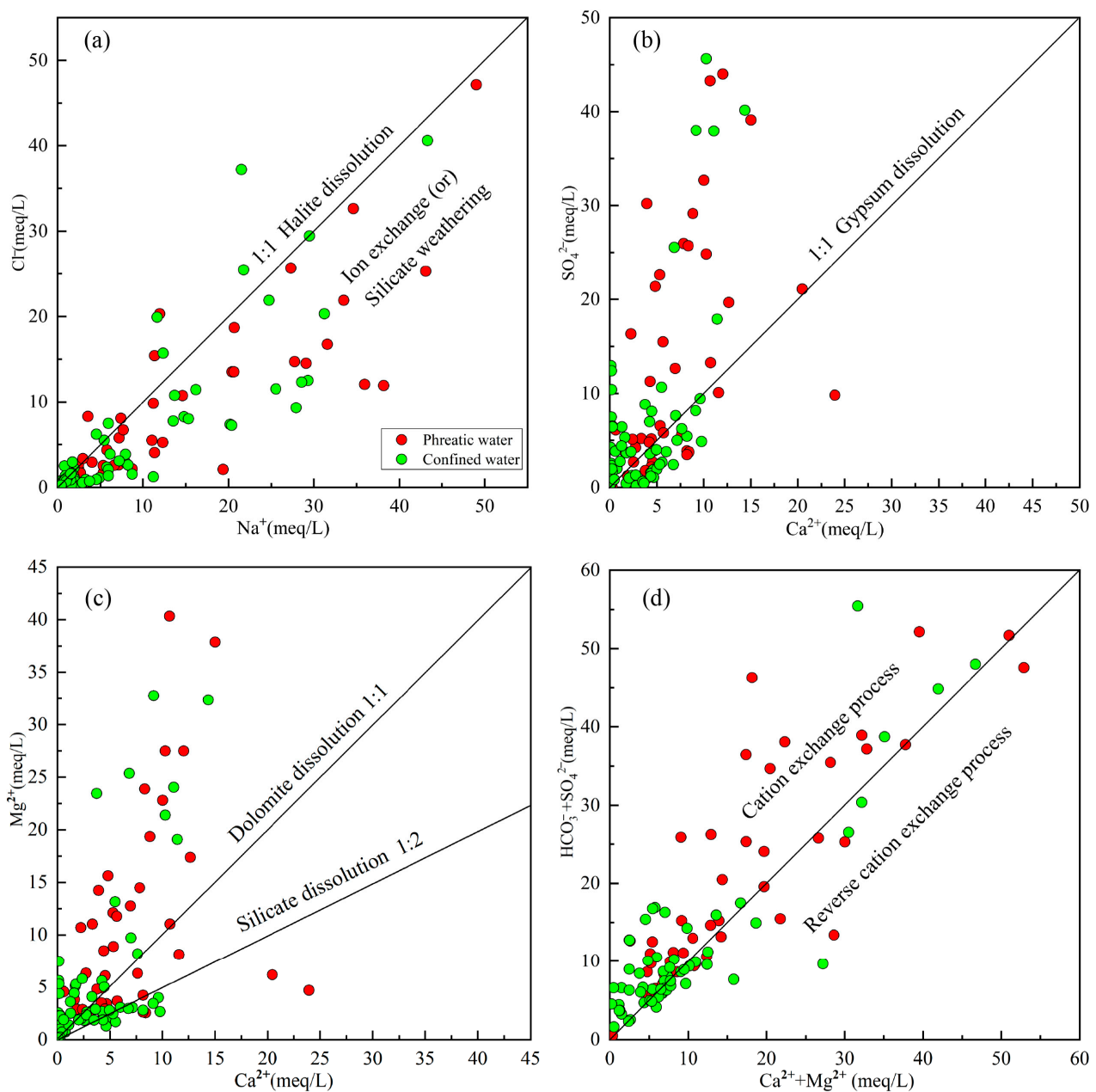


Figure 9. Scatter plot of major ion concentrations in phreatic and confined groundwater (a) Cl^- versus Na^+ , (b) SO_4^{2-} versus Ca^{2+} , (c) Mg^{2+} versus Ca^{2+} , (d) $\text{HCO}_3^- + \text{SO}_4^{2-}$ versus $\text{Ca}^{2+} + \text{Mg}^{2+}$.

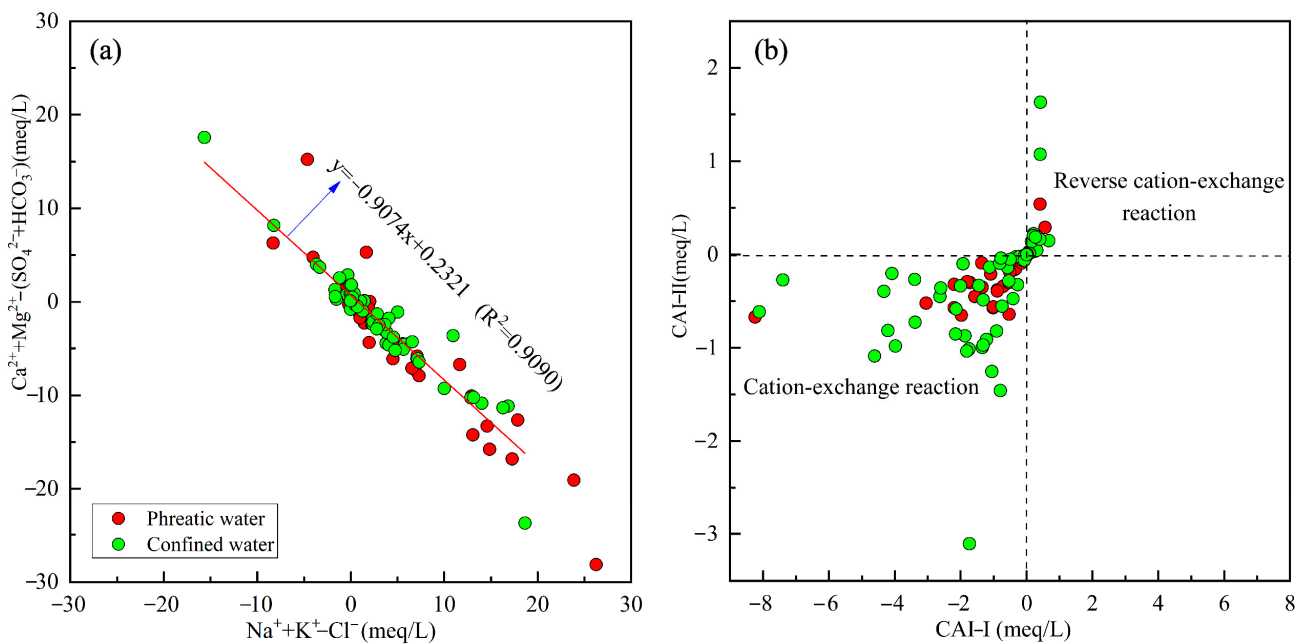


Figure 10. Plots of (a) $(\text{Ca}^{2+} + \text{Mg}^{2+} - \text{HCO}_3^- - \text{SO}_4^{2-})$ versus $(\text{Na}^+ + \text{K}^+ - \text{Cl}^-)$, (b) CAI-I versus CAI-II.

The saturation index (SI) is one of the most widely used metrics in groundwater hydrochemical studies, and SI values can reliably reveal the dissolved state of specific minerals. When the SI values are <0 , $=0$ and >0 , it indicates the minerals are in dissolved, equilibrium and saturated states in the groundwater, respectively. In this research, the SI values of calcite, dolomite, gypsum, anhydrite, aragonite and halite in phreatic and confined groundwater were calculated to further reveal the material sources of hydrogeochemical components using PHREEQC2.11 software, and the spatial distributions of the saturation indices of minerals were shown in Figures 11 and 12. The SI values of aragonite, calcite, and dolomite in phreatic groundwater varied from -1.29 – 0.69 , -1.15 – 0.84 , and -2.53 – 2.45 , respectively. Figure 11b–d shows that aragonite, calcite, and dolomite minerals were oversaturated within a broad range of phreatic groundwaters in the southern Hebei province, and dissolved only in the northwestern mountainous zone. This evidenced the results of Figure 8c, indicating that dissolution of carbonates did not have the dominant role in controlling the hydrogeochemical components of the phreatic groundwater. The SI values for halite, gypsum and anhydrite were -9.46 – 4.44 , -3.88 – -0.31 and -4.19 – -0.61 , respectively, indicating the three minerals were dissolved in phreatic aquifer and showed an increasing trend from the western mountainous areas to the eastern plains (Figure 11a,e,f).

In confined groundwater, the SI values ranged from -0.93 – 0.74 , -0.79 – 0.88 and -4.20 – 2.62 for aragonite, calcite and dolomite, respectively. Aragonite and calcite gradually evolved from the oversaturated state to the dissolved state along the runoff path from west to east (Figure 12b,c). Different from phreatic groundwater, carbonate minerals (aragonite and calcite) in confined groundwater were dissolved in the eastern plain, implying that dissolution of aragonite and calcite had potential contributions to the hydrogeochemical component of confined groundwater. The SI values for anhydrite, gypsum and halite were in the range of -4.64 to -0.70 , -4.33 to -0.40 and -8.67 to -4.55 , respectively, suggesting that dissolution of these three minerals had a significant contributing role in the chemical composition of confined groundwater. The dissolution degree of gypsum and anhydrite minerals gradually increased along the path of the confined groundwater runoff, while the dissolution degree of halite gradually decreased (Figure 12a,e,f). Consequently, it is comprehensively concluded that the dissolution of aragonite, calcite, gypsum, anhydrite and halite are the main material source of ions in confined groundwater.

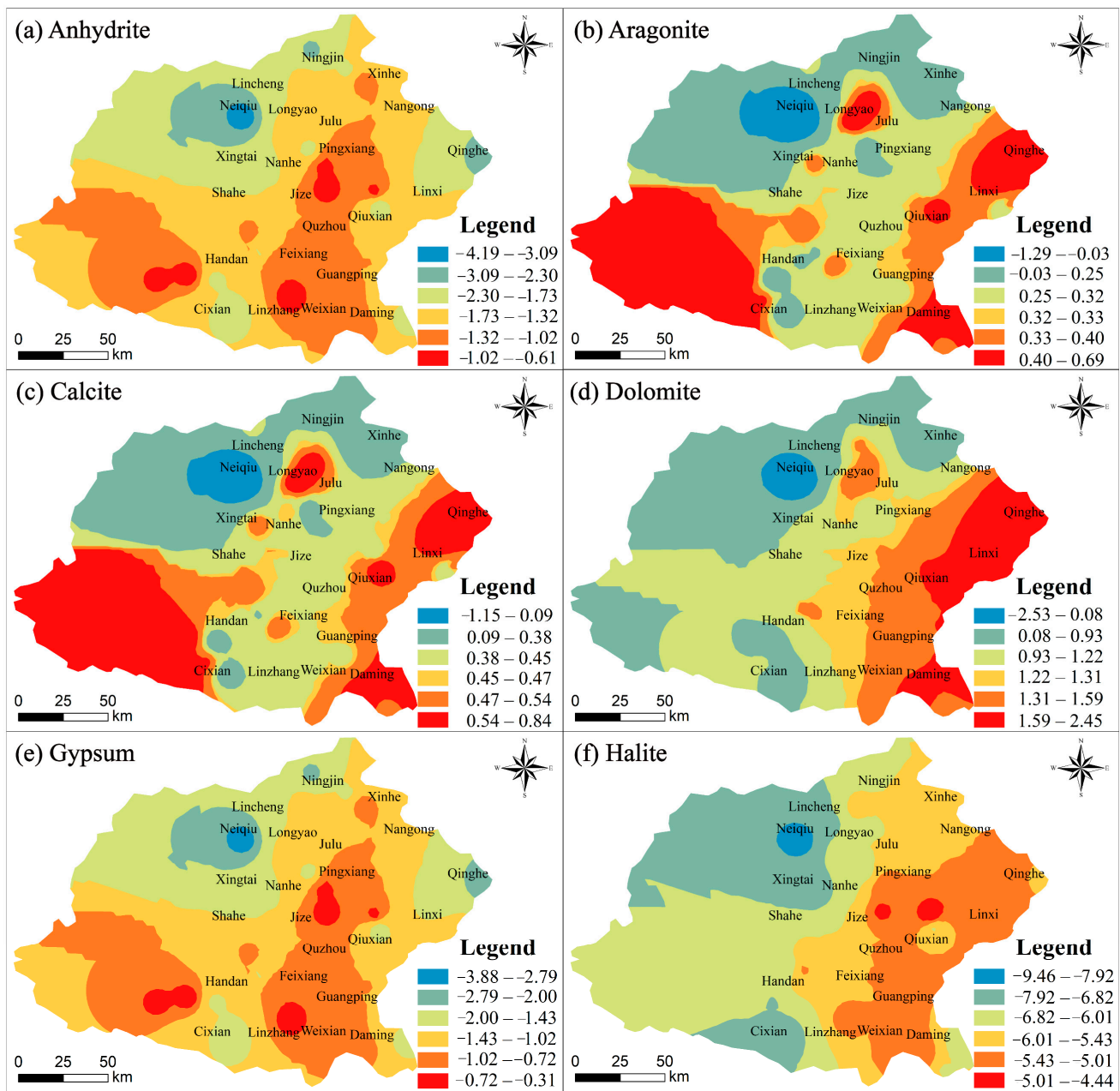


Figure 11. Spatial distribution of main mineral saturation index (SI) in phreatic water samples.

4.2.2. Anthropogenic Factors

In addition to natural processes, the hydrogeochemical components of groundwater are also greatly affected by various anthropogenic activities [47–49]. Nitrate was widely used to reveal the effects of anthropogenic activities on groundwater, and the hydrogeochemical limit for nitrate levels in natural groundwater is 10 mg/L. Figure 13a showed that approximately 27% of phreatic and 15% of confined water samples had nitrate concentrations exceeding 10 mg/L (Figure 13a), suggesting a potential anthropogenic influence on groundwater hydrochemistry. As an important anion in groundwater, Cl^- may be derived from external anthropogenic inputs besides halite dissolution by natural processes. In Figure 13a, a positive correlation was observed between NO_3^- and Cl^- in groundwater samples beyond the nitrate geochemical baseline, meaning that these two ionic materials were of similar origin and anthropogenic input. In Figure 13b, $(\text{NO}_3^- + \text{Cl}^-)/\text{HCO}_3^-$ and TDS were positively correlated in groundwater samples, confirming the input of NO_3^- and Cl^- components in groundwater caused by external anthropogenic activities.

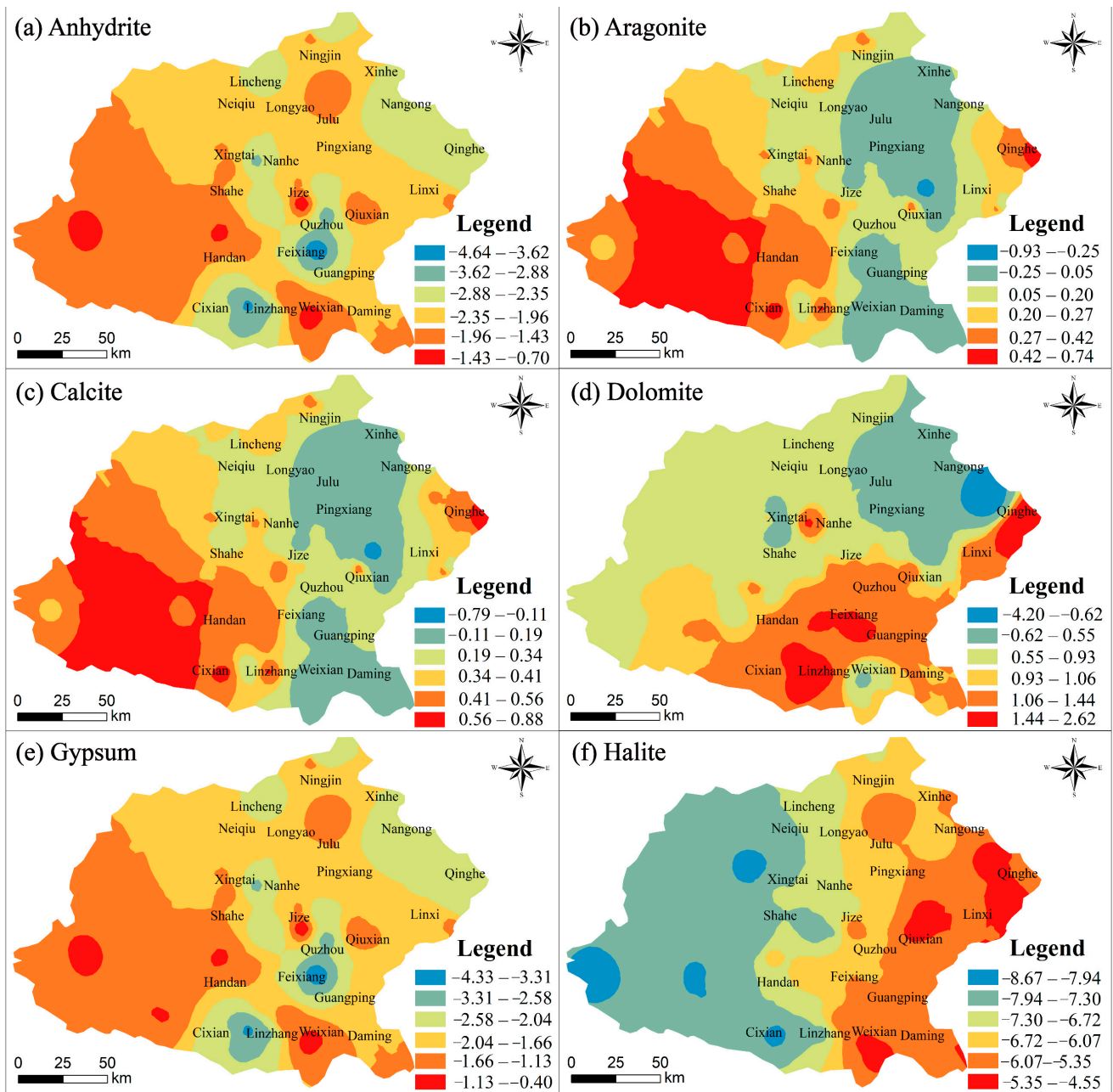


Figure 12. Saturation index plots with selected minerals in confined water.

The spatial distribution maps of nitrate concentrations revealed that NO_3^- concentrations in phreatic and confined aquifers within the eastern plain of the region were lower than the geochemical baseline of the natural groundwater (Figure 14), suggesting that NO_3^- in this region derived from hydrogeochemical processes rather than external inputs of anthropogenic activities. In the study area, phreatic groundwater samples with nitrate concentration exceeding 10 mg/L were mainly situated in Xingtai, Handan, Cixian, Ningjin and Nanhe counties. This indicated that phreatic groundwater in these areas was influenced by anthropogenic activities such as irrigation backseepage, garbage dumping and urban sewage discharge. Confined groundwater samples with NO_3^- concentrations exceeding the baseline, were observed concentrated in the western premontane floodplain area, which may potentially be influenced by irrigation re-infiltration from agricultural practices and deep mining activities in this region. Therefore, protective measures are recommended in the urban areas of Xingtai and Handan as well as in the pre-mountain alluvial plain area to control potential sources of contamination such as municipal sewage,

surface solid wastes, and irrigation back-seepage from seeping into the aquifer and leading to deterioration of water quality. In addition, it is also recommended to introduce various isotopes such as $^{18}\text{O}-\text{NO}_3$ and $^{15}\text{N}-\text{NO}_3$ to distinguish the effects of groundwater quality deterioration caused by different human activities.

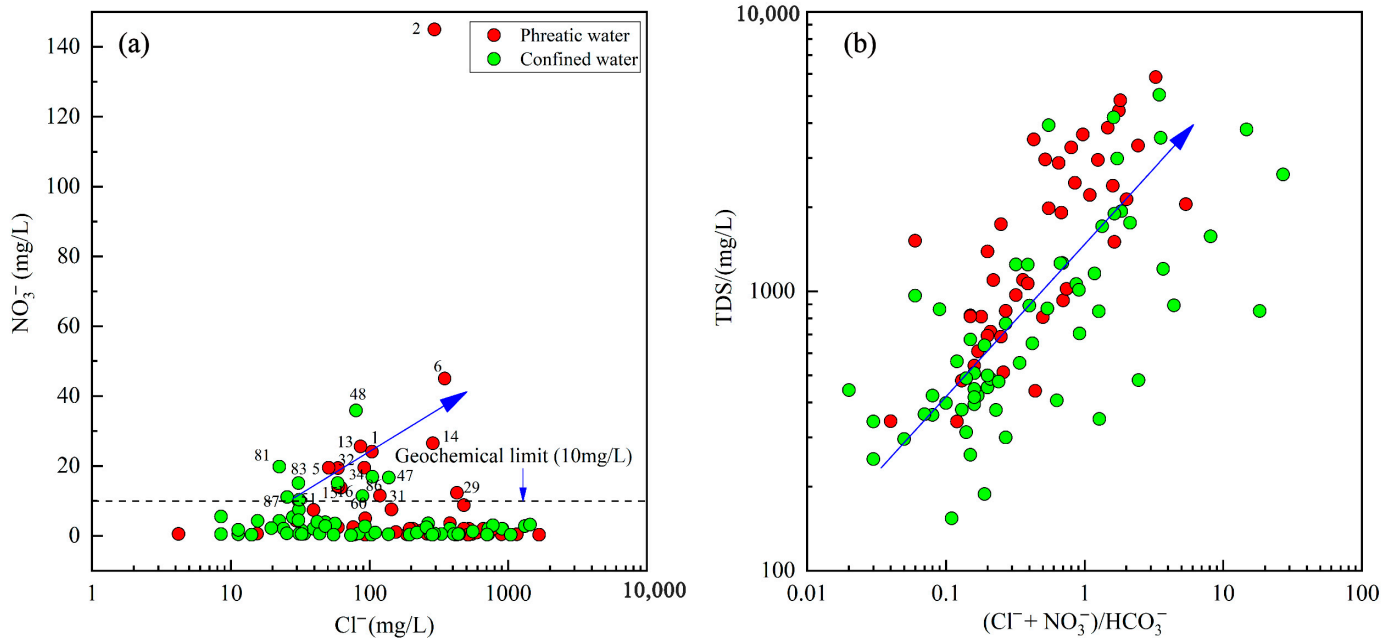


Figure 13. Correlation diagrams of (a) Cl^- vs. NO_3^- , and (b) TDS vs. $(\text{NO}_3^- + \text{Cl}^-)/\text{HCO}_3^-$.

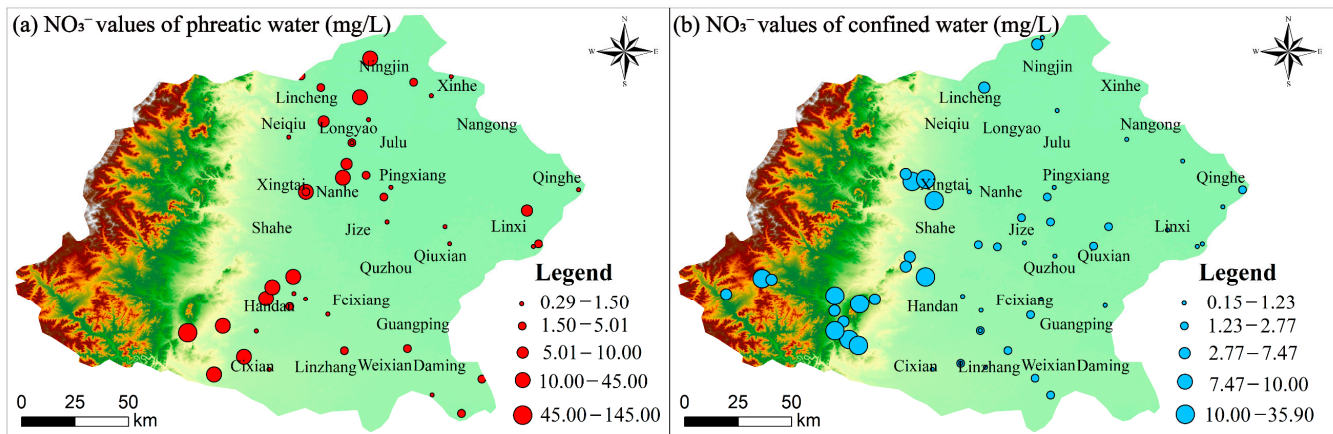


Figure 14. Spatial pattern map of NO_3^- for (a) phreatic groundwater and (b) confined groundwater.

4.3. Source Statistical Analysis

To identify the relationships between the different variables in groundwater, the correlation coefficient matrices of 12 different variables in phreatic and confined groundwater samples (Table 2) were calculated using Origin version 2021 software. The Pearson correlation coefficient revealed that K^+ , HCO_3^- , NO_3^- and F^- were weakly correlated with each indicator in groundwater samples. This indicated that K^+ , HCO_3^- , NO_3^- and F^- were relatively independent influencing factors among the 12 selected indicators and could reflect the environmental quality of groundwater from different aspects. However, the correlation coefficients between TH, TDS, Na^+ , Ca^{2+} , Mg^{2+} , Cl^- and SO_4^{2-} were mostly above 0.5, indicating a high correlation and information overlap among the indicators. For phreatic water samples, strong positive correlations were observed for $\text{TDS}-\text{Na}^+$, $\text{TDS}-\text{Mg}^{2+}$, $\text{TDS}-\text{Cl}^-$, $\text{TDS}-\text{SO}_4^{2-}$ and $\text{TDS}-\text{TH}$, indicating that the presence of Na^+ , Mg^{2+} , Cl^- , SO_4^{2-} and TH greatly influenced the TDS. Meanwhile, significant positive correlations of Na^+ ,

SO₄²⁻, TH and TDS indicated geological weathering and hydrogeochemical evolution of high ion concentrations which might be related to human activities. Notably, the significant positive correlations between Na⁺-Cl⁻ (r = 0.84), Na⁺-SO₄²⁻ (r = 0.86) and Cl⁻-SO₄²⁻ (r = 0.86) indicate the potential influence of evaporation and agricultural activities on shallow groundwater systems. Except for pH and Ca²⁺, none of the studied variables were observed with a significant correlation with F⁻.

Table 2. Correlation coefficient matrix of physicochemical parameters of phreatic and confined groundwater.

	TH	TDS	pH	Na ⁺	K ⁺	Ca ²⁺	Mg ²⁺	Cl ⁻	SO ₄ ²⁻	HCO ₃ ⁻	NO ₃ ⁻	F ⁻
Phreatic groundwater samples (n = 45)												
TH	1											
TDS	0.91 **	1										
pH	-0.47 **	-0.31 *	1									
Na ⁺	0.67 **	0.91 **	-0.11	1								
K ⁺	0.17	0.10			1							
Ca ²⁺	0.73 **	0.50 **	-0.45 **	0.16	0.28	1						
Mg ²⁺	0.93 **	0.93 **	-0.38 **	0.80 **		0.44 **	1					
Cl ⁻	0.87 **	0.93 **	-0.21	0.84 **	0.17	0.43 **	0.91 **	1				
SO ₄ ²⁻	0.89 **	0.97 **	-0.30 *	0.86 **		0.50 **	0.91 **	0.86 **	1			
HCO ₃ ⁻	0.20	0.37 *	-0.37 *	0.52 **	-0.19	-0.11	0.32 *	0.20	0.26	1		
NO ₃ ⁻				-0.24	0.45 **	0.59 **	-0.19	-0.12	-0.12	-0.18	1	
F ⁻		0.11	0.49 **	0.28	-0.19	-0.33 *				0.26	-0.24	1
Confined groundwater samples (n = 62)												
TH	1											
TDS	0.90 **	1										
pH	-0.51 **	-0.22	1									
Na ⁺	0.61 **	0.89 **	0.15	1								
K ⁺					1							
Ca ²⁺	0.82 **	0.58 **	-0.74 **	0.18	0.21	1						
Mg ²⁺	0.97 **	0.94 **	-0.35 **	0.73 **		0.64 **	1					
Cl ⁻	0.78 **	0.88 **		0.83 **		0.39 **	0.86 **	1				
SO ₄ ²⁻	0.88 **	0.95 **	-0.26 *	0.79 **		0.63 **	0.89 **	0.70 **	1			
HCO ₃ ⁻	0.28 *	0.24	-0.46 **	0.15		0.28 *	0.24		0.23	1		
NO ₃ ⁻		-0.19	-0.34 **	-0.37 **	0.28	0.38 **	-0.19	-0.25 *	-0.15		1	
F ⁻		0.26 *	0.29 *	0.55 **	-0.14	-0.29 *		0.29 *	0.15	0.20	-0.29 *	1

Note: ** and * indicate significant correlation at the 0.01 and 0.05 levels (2-tailed), respectively.

The correlation matrix results for the confined groundwater samples were similar to those for the phreatic groundwater samples. TH-TDS, Na⁺-TDS, Mg²⁺-TDS, Cl⁻-TDS, SO₄²⁻-TDS, Ca²⁺-TH, Mg²⁺-TH, SO₄²⁻-TH, Na⁺-Cl⁻, Mg²⁺-Cl⁻ and Mg²⁺-SO₄²⁻ were strongly correlated in confined groundwater. Na⁺-TH, Ca²⁺-TDS, Na⁺-Mg²⁺, Ca²⁺-Mg²⁺, Ca²⁺-SO₄²⁻ and Cl⁻-SO₄²⁻ were observed to have significant positive correlations at the 0.01 level. It was notable that the correlation of Na-Ca (r = 0.18) was poor, which may be caused by cation exchange. In addition, the weak correlation of NO₃⁻-Ca²⁺ (r = 0.38) and the negative correlation of NO₃⁻-Na⁺ (r = -0.37) suggests that the source of NO₃⁻ might derive from agricultural activities.

Hierarchical cluster analysis (HCA) was an effective method to analyze the source and influencing factors of hydrogeochemical parameters [50–52]. In this research, the similarity of hydrogeochemical parameters was measured by the Ward linkage method and Euclidean distance squared. The dendrogram generated by HCA divided the physicochemical parameters into three clusters, and the clustering results for phreatic and confined water samples are shown in Figure 15a,b. Cluster 1 for phreatic and confined water, mainly included Na⁺, Mg²⁺, HCO₃⁻, SO₄²⁻, Cl⁻, TH, TDS, indicating mineral dissolution and rock weathering processes. Cluster 2 included pH and F⁻, indicating that a slightly alkaline pH environment is conducive to the dissolution and enrichment of F⁻. Cluster 3 comprised K⁺, Ca²⁺, NO₃⁻, suggesting that K⁺ and NO₃⁻ in groundwater may have originated from local agricultural activities.

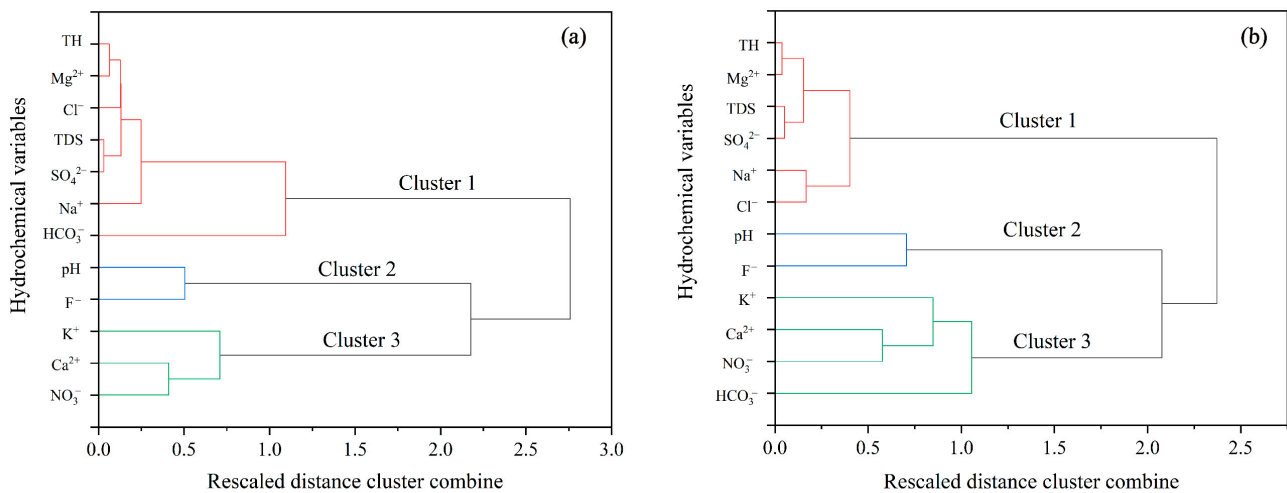


Figure 15. Dendrogram for (a) phreatic and (b) confined groundwater samples showing clustering of hydrogeochemical variables.

4.4. Groundwater Quality Evaluation

Groundwater quality evaluation is an essential component of groundwater resource evaluation and protection. Through water quality assessment, it is possible to understand and grasp the change trend of water quality, and provide a scientific basis for the utilization, protection, planning and management of groundwater resources. EWQI is an evaluation model that comprehensively reflects the water quality condition through the weights of several physicochemical parameters. Based on groundwater quality monitoring data, EWQI was used to comprehensively evaluate the water quality conditions of phreatic and confined aquifers in southern Hebei Province. Twelve parameters in groundwater were selected to participate in EWQI calculation and evaluation, including pH, TH, TDS, Cl⁻, SO₄²⁻, Ca²⁺, K⁺, Mg²⁺, Na⁺, NO₃⁻, HCO₃⁻ and F⁻. The information entropy (e_j) and entropy weight (w_j) of each indicator involved in the calculation of the water quality index are presented in Table 3.

Table 3. Information entropy and entropy weight of each physicochemical parameter in groundwater.

Index	Category	TH	TDS	pH	Na ⁺	K ⁺	Ca ²⁺	Mg ²⁺	Cl ⁻	SO ₄ ²⁻	HCO ₃ ⁻	NO ₃ ⁻	F ⁻
Information entropy (e _j)	Phreatic groundwater	0.929	0.927	0.918	0.886	0.918	0.928	0.899	0.874	0.881	0.963	0.676	0.909
	Confined groundwater	0.891	0.874	0.921	0.849	0.920	0.895	0.847	0.804	0.824	0.959	0.796	0.898
Entropy weight (w _j)	Phreatic groundwater	0.055	0.057	0.063	0.088	0.064	0.056	0.078	0.097	0.092	0.029	0.250	0.070
	Confined groundwater	0.071	0.083	0.052	0.099	0.053	0.069	0.101	0.129	0.115	0.027	0.134	0.067

The EWQI values of phreatic and confined groundwater in the southern Hebei Province were 8.64~3519 and 9.45~2724 as calculated by Equations (3)–(9). For phreatic groundwater samples, 6.67% were excellent, 11.11% were good, 13.33% were medium, 8.89% were poor and 60.00% were extremely poor. While for confined groundwater samples, 20.97% were excellent, 29.03% were good, 14.53% were medium, 9.67% were poor and 25.80% were extremely poor. In general, groundwater with good or excellent quality grades is suitable for drinking, otherwise, other rankings of groundwater need to be treated before being utilized as drinking water. In this survey, a total of 17.78% of shallow phreatic groundwater and 50.00% of deep confined groundwater meet the quality for drinking purposes, and the quality of deep confined groundwater is significantly better than phreatic groundwater. The spatial distribution patterns of the EWQI values of phreatic and deep confined groundwater samples in the southern Hebei Province were plotted in Figure 16. High EWQI values for phreatic groundwater were mainly concentrated in the south and northeast, while high EWQI confined groundwaters were centered in the southeast. Therefore, attention should be paid to areas with high EWQI values, and groundwater quality

should be improved by strengthening the groundwater environmental monitoring and improving groundwater protection and management measures.

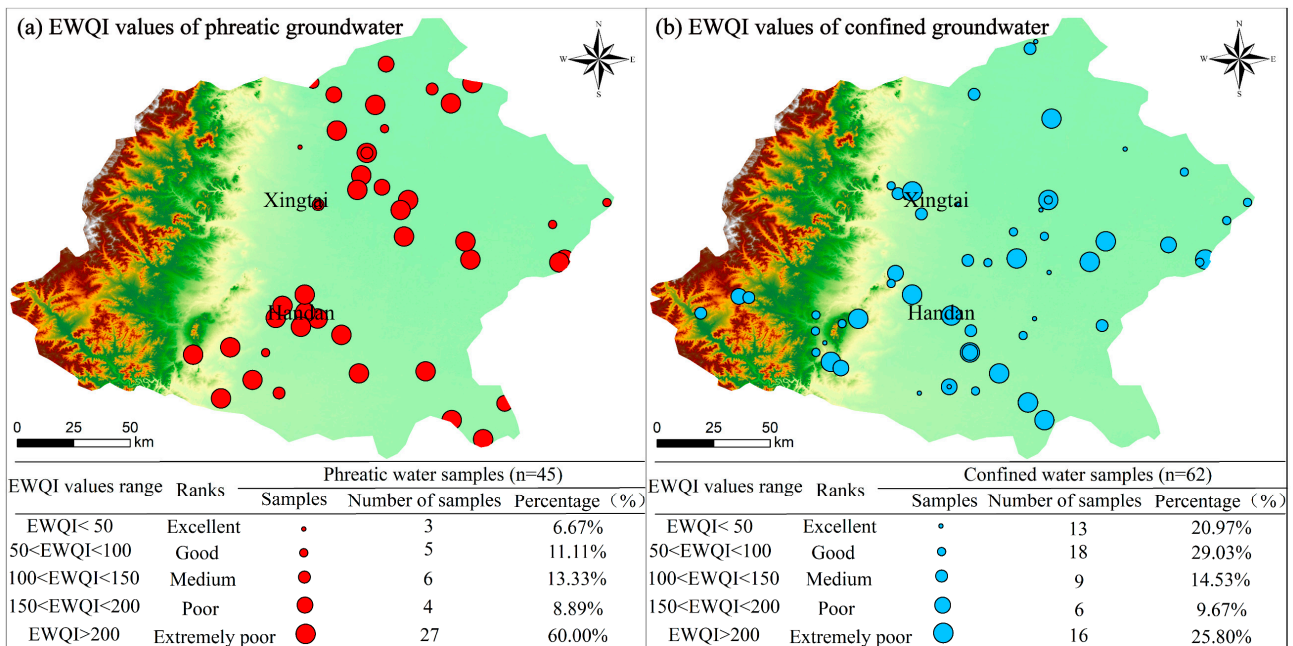


Figure 16. (a) Spatial pattern map of EWQI values for phreatic groundwater; (b) Spatial pattern map of EWQI values for confined groundwater.

In order to further analyze the influence of groundwater indicators on EWQI, Pearson correlation analysis was conducted between 12 selected indicators and EWQI, and the results are shown in Figure 17. The weak significance of K^+ , HCO_3^- , NO_3^- , and F^- with EWQI in the phreatic and confined aquifers indicated that K^+ , HCO_3^- , NO_3^- , and F^- had little influence on the environmental quality of groundwater. Figure 16 revealed that TH, TDS, Mg^{2+} , Cl^- and SO_4^{2-} were all significantly correlated with the EWQI of both phreatic and confined water, indicating that TH, TDS, Mg^{2+} , Cl^- and SO_4^{2-} have a significant influence on groundwater quality. Hence, in future groundwater quality monitoring, it is necessary to optimize the monitoring indicators and focus on the indicators that contribute more to the groundwater environmental quality, so as to reduce the monitoring costs.

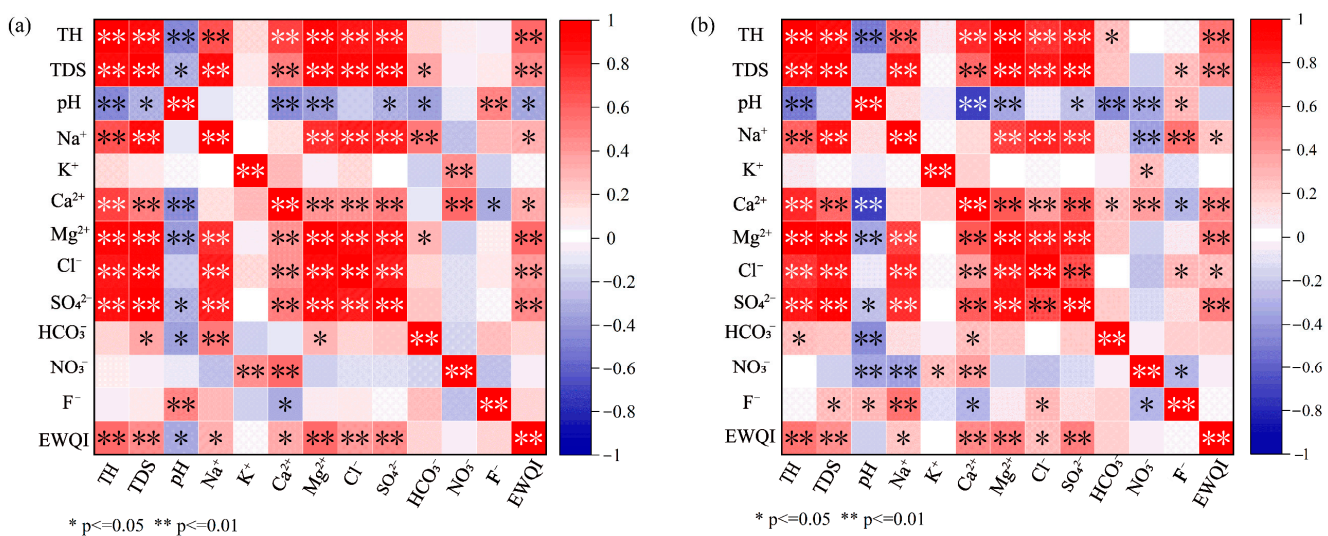


Figure 17. Correlation between EWQI and (a) phreatic and (b) confined groundwater quality indexes.

4.5. Corresponding Protection and Management Measures

Groundwater quality assessment is the basis of groundwater resource protection and the scientific basis of groundwater pollution prevention. According to the above groundwater quality evaluation results, the following measures should be taken to strengthen the protection and sustainable utilization of groundwater resources in southern Hebei Province.

- (1) Groundwater wells with EWQI values exceeding 100 should be stopped until remedial action is taken.
- (2) The use of nitrate-rich fertilizer and stockpiling of the waste ore and garbage should be reduced in the western piedmont plain, and appropriate ecological measures should be used to reduce nitrate concentrations.
- (3) Groundwater filtration equipment should be installed to reduce the concentrations of Mg^{2+} , SO_4^{2-} , Cl^- , TH and TDS values in groundwater with high EWQI.
- (4) Real-time water quality monitoring systems and early warning platforms to enhance monitoring capabilities should be established.
- (5) A sound and scientific water resources management system, and rational plan for the development and utilization of groundwater should be established.

5. Conclusions

In this study, the hydrogeochemical characteristics and control mechanisms of shallow phreatic and deep confined groundwater in the southern plain of Hebei Province were discussed in depth. The entropy variable weight water quality index was also introduced to evaluate the feasibility of groundwater for domestic drinking purposes. The main conclusions of this study were as follows:

Both phreatic and deep karst confined groundwater in the plains of southern Hebei Province were weakly alkaline freshwater, and karst confined groundwater was fresher than phreatic groundwater. The main anion abundance order in aquifer groundwater was $SO_4^{2-} > HCO_3^- > Cl^-$, and the cation order was $Na^+ > Ca^{2+} > Mg^{2+} > K^+$. The water chemistry of phreatic groundwater was mainly HCO_3 -Ca-Mg and Ca-Mg- SO_4 -Cl, and the karst confined groundwater was HCO_3 -Ca-Mg and Na-Cl- SO_4 type water. The hydrochemical composition of phreatic groundwater was dominated by gypsum, anhydrite, halite mineral dissolution and cation exchange, and was also potentially influenced by evapotranspiration and anthropogenic activities. The deep karst confined groundwater was dominated by the dissolution of carbonate minerals (dolomite, calcite, aragonite) and sulfate mineral. The results of groundwater quality evaluation showed that phreatic and confined groundwater meeting the purpose of drinking water in the study area accounted for 17.78% and 50.00%, respectively. Phreatic groundwater samples with poor water quality were mainly concentrated in the Handan urban area and the eastern region of Xingtai City. The quality rankings of confined groundwater samples were mainly excellent and good, and the water quality was significantly better than phreatic groundwater. The results of EWQI and correlation analyses revealed that the main physicochemical indicators affecting water quality were TH, TDS, Mg^{2+} , Cl^- , and SO_4^{2-} . In general, it is recommended to give priority to the utilization of karst confined groundwater for domestic and drinking purposes, and corresponding protection and management measures should be taken for the phreatic groundwater to realize the sustainable use of local groundwater resources.

Author Contributions: Conceptualization, L.Z. and D.D.; methodology, D.D., L.Z. and S.L.; software, L.Z. and J.Z.; formal analysis, S.L.; investigation, M.Y., J.Z. and G.H.; data curation, D.D.; writing—original draft preparation, L.Z. and D.D.; writing—review and editing, L.Z. and D.D.; visualization, H.L.; supervision, D.D.; project administration, D.D.; funding acquisition, D.D. All authors have read and agreed to the published version of the manuscript.

Funding: This study was funded by the Key Research and Development Program of Hebei Province: Key Technology Research on the Cause Analysis and Precise Control of groundwater Funnel in Hebei Province (21373901D) and Basic Scientific Research Funds of China University of Mining and Technology (Beijing)—Top Innovative Talents Cultivation Fund for Doctoral Postgraduates (grant no. BBJ2023020).

Data Availability Statement: The data that support the findings of this study are available from the corresponding author upon reasonable request.

Acknowledgments: The authors are grateful to the China Environmental Monitoring Institute and North China Nonferrous Metals for their help in data collection and field investigation. Special thanks to the editor and anonymous reviewers for their important comments and valuable suggestions.

Conflicts of Interest: The authors declare no conflict of interest.

References

1. Liu, Y.; Wang, P.; Ruan, H.; Wang, T.; Yu, J.; Cheng, Y.; Kulmatov, R. Sustainable Use of Groundwater Resources in the Transboundary Aquifers of the Five Central Asian Countries: Challenges and Perspectives. *Water* **2020**, *12*, 2101. [[CrossRef](#)]
2. Gao, F.; Wang, H.; Liu, C. Long-term assessment of groundwater resources carrying capacity using GRACE data and Budyko model. *J. Hydrol.* **2020**, *588*, 125042. [[CrossRef](#)]
3. Siebert, S.; Burke, J.; Faures, J.M.; Frenken, K.; Hoogeveen, J.; Döll, P.; Portmann, F.T. Groundwater use for irrigation—A global inventory. *Hydrol. Earth Syst. Sci.* **2010**, *14*, 1863–1880. [[CrossRef](#)]
4. Gleeson, T.; Befus, K.M.; Jasechko, S.; Luijendijk, E.; Cardenas, M.B. The global volume and distribution of modern groundwater. *Nat. Geosci.* **2015**, *9*, 161–167. [[CrossRef](#)]
5. Wang, H.; Jia, G. Satellite-based monitoring of decadal soil salinization and climate effects in a semi-arid region of China. *Adv. Atmos. Sci.* **2012**, *29*, 1089–1099. [[CrossRef](#)]
6. Li, M.; Xie, Y.; Dong, Y.; Wang, L.; Zhang, Z. Review: Recent progress on groundwater recharge research in arid and semiarid areas of China. *Hydrogeol. J.* **2023**, *278*, 1–22. [[CrossRef](#)]
7. Arabameri, A.; Rezaei, K.; Cerda, A.; Lombardo, L.; Rodrigo-Comino, J. GIS-based groundwater potential mapping in Shahroud plain, Iran. A comparison among statistical (bivariate and multivariate), data mining and MCDM approaches. *Sci. Total Environ.* **2019**, *658*, 160–177. [[CrossRef](#)]
8. Valdes-Abellan, J.; Pardo, M.A.; Jodar-Abellan, A.; Pla, C.; Fernandez-Mejuto, M. Climate change impact on karstic aquifer hydrodynamics in southern Europe semi-arid region using the KAGIS model. *Sci. Total Environ.* **2020**, *723*, 138110. [[CrossRef](#)]
9. Han, S.; Yang, Y.; Fan, T.; Xiao, D.; Moiwo, J.P. Precipitation-runoff processes in Shimen hillslope micro-catchment of Taihang Mountain, north China. *Hydrol. Process.* **2012**, *26*, 1332–1341. [[CrossRef](#)]
10. Gastélum, J.R.; Cullom, C. Application of the Colorado River Simulation System Model to Evaluate Water Shortage Conditions in the Central Arizona Project. *Water Resour. Manag.* **2013**, *27*, 2369–2389. [[CrossRef](#)]
11. Sun, Y.; Liu, N.; Shang, J.; Zhang, J. Sustainable utilization of water resources in China: A system dynamics model. *J. Clean. Prod.* **2017**, *142*, 613–625. [[CrossRef](#)]
12. Chen, X.; Li, F.; Li, X.; Hu, Y.; Hu, P. Evaluating and mapping water supply and demand for sustainable urban ecosystem management in Shenzhen, China. *J. Clean. Prod.* **2020**, *251*, 119754. [[CrossRef](#)]
13. Zhang, J.; Chen, L.; Hou, X.; Li, J.; Ren, X.; Lin, M.; Zhang, M.; Wang, Y.; Tian, Y. Effects of multi-factors on the spatiotemporal variations of deep confined groundwater in coal mining regions, North China. *Sci. Total Environ.* **2022**, *823*, 153741. [[CrossRef](#)] [[PubMed](#)]
14. Bowell, R.J. Hydrogeochemistry of the Tsumeb Deposit: Implications for Arsenate Mineral Stability. *Rev. Mineral. Geochem.* **2014**, *79*, 589–627. [[CrossRef](#)]
15. Yang, Q.; Li, Z.; Ma, H.; Wang, L.; Martin, J.D. Identification of the hydrogeochemical processes and assessment of groundwater quality using classic integrated geochemical methods in the Southeastern part of Ordos basin, China. *Environ. Pollut.* **2016**, *218*, 879–888. [[CrossRef](#)]
16. Hoaghia, M.A.; Moldovan, A.; Kovacs, E.; Mirea, I.; Kenesz, M.; Brad, T.; Cadar, O.; Micle, V.; Levei, E.; Moldovan, O. Water Quality and Hydrogeochemical Characteristics of Some Karst Water Sources in Apuseni Mountains, Romania. *Water* **2021**, *13*, 857. [[CrossRef](#)]
17. Chen, S.; Tang, Z.; Wang, J.; Wu, J.; Yang, C.; Kang, W.; Huang, X. Multivariate Analysis and Geochemical Signatures of Shallow Groundwater in the Main Urban Area of Chongqing, Southwestern China. *Water* **2020**, *12*, 2833. [[CrossRef](#)]
18. Nobre, R.C.; Nobre, M.M. Natural attenuation of chlorinated organics in a shallow sand aquifer. *J. Hazard. Mater.* **2004**, *110*, 129–137. [[CrossRef](#)]
19. Négrel, P.; Lemièrre, B.; Machard de Grammont, H.; Billaud, P.; Sengupta, B. Hydrogeochemical processes, mixing and isotope tracing in hard rock aquifers and surface waters from the Subarnarekha River Basin, (east Singhbhum District, Jharkhand State, India). *Hydrogeol. J.* **2007**, *15*, 1535–1552. [[CrossRef](#)]

20. Liu, F.; Wang, S.; Wang, L.; Shi, L.; Song, X.; Zhen, P. Coupling hydrochemistry and stable isotopes to identify the major factors affecting groundwater geochemical evolution in the Heilongdong Spring Basin, North China. *J. Geochem. Explor.* **2019**, *205*, 106352. [[CrossRef](#)]
21. Özdemir, Ö. Application of Multivariate Statistical Methods for Water Quality Assessment of Karasu-Sarmisakli Creeks and Kizilirmak River in Kayseri, Turkey. *Pol. J. Environ. Stud.* **2016**, *25*, 1149–1160. [[CrossRef](#)]
22. Li, M.; Liu, Z.; Zhang, M.; Chen, Y. A workflow for spatio-seasonal hydro-chemical analysis using multivariate statistical techniques. *Water Res.* **2021**, *188*, 116550. [[CrossRef](#)] [[PubMed](#)]
23. Zhang, L.; Dong, D.; Lv, S.; Ding, J.; Yan, M.; Han, G. Spatial evolution analysis of groundwater chemistry, quality, and fluoride health risk in southern Hebei Plain, China. *Environ. Sci. Pollut. Res.* **2023**, *30*, 61032–61051. [[CrossRef](#)]
24. Zhang, H.; Singh, V.P.; Sun, D.; Yu, Q.; Cao, W. Has water-saving irrigation recovered groundwater in the Hebei Province plains of China? *Int. J. Water Resour. Dev.* **2016**, *33*, 534–552. [[CrossRef](#)]
25. Yu, L.; Ling, M.; Chen, F.; Ding, Y.; Lv, C. Practices of groundwater over-exploitation control in Hebei Province. *Water Policy* **2020**, *22*, 591–601.
26. Yuan, Z.; Shen, Y. Estimation of agricultural water consumption from meteorological and yield data: A case study of Hebei, North China. *PLoS ONE* **2013**, *8*, e58685. [[CrossRef](#)]
27. Xu, Y.; Mo, X.; Cai, Y.; Li, X. Analysis on groundwater table drawdown by land use and the quest for sustainable water use in the Hebei Plain in China. *Agric. Water Manag.* **2005**, *75*, 38–53. [[CrossRef](#)]
28. Hu, X.; Shi, L.; Zeng, J.; Yang, J.; Zha, Y.; Yao, Y.; Cao, G. Estimation of actual irrigation amount and its impact on groundwater depletion: A case study in the Hebei Plain, China. *J. Hydrol.* **2016**, *543*, 433–449. [[CrossRef](#)]
29. Feng, W.; Zhong, M.; Lemoine, J.M.; Biancale, R.; Hsu, H.T.; Xia, J. Evaluation of groundwater depletion in North China using the Gravity Recovery and Climate Experiment (GRACE) data and ground-based measurements. *Water Resour. Res.* **2013**, *49*, 2110–2118. [[CrossRef](#)]
30. Wang, Y.; Cheng, L.; Tian, H.; Liu, X. Water supply eco-economic benefit evaluation of middle route of south-to-north water diversion project in Hebei Water-recipient Area. *IOP Conf. Ser. Earth Environ. Sci.* **2018**, *191*, 012064. [[CrossRef](#)]
31. Wang, M.; Liao, L.; Zhang, X.; Li, Z.; Xia, Z.; Cao, W. Adsorption of low-concentration ammonium onto vermiculite from Hebei Province, China. *Clays Clay Miner.* **2011**, *59*, 459–465. [[CrossRef](#)]
32. Zhang, Q.; Han, X.; Li, J.; Zhao, J.; Zhou, W.; Gao, W. The Study on Environmental Evolved Characteristic of Sandy Coast. *Appl. Mech. Mater.* **2012**, *226–228*, 1170–1173. [[CrossRef](#)]
33. Li, G.; Han, T.; Li, X. Groundwater environmental degradation mechanism and countermeasures in the plain area of Xingtai City. *Groundwater* **2011**, *33*, 63–66.
34. Charlton, S.R.; Parkhurst, D.L. Modules based on the geochemical model PHREEQC for use in scripting and programming languages. *Comput. Geosci.* **2011**, *37*, 1653–1663. [[CrossRef](#)]
35. Islam, A.R.M.T.; Ahmed, N.; Bodrud-Doza, M.; Chu, R. Characterizing groundwater quality ranks for drinking purposes in Sylhet district, Bangladesh, using entropy method, spatial autocorrelation index, and geostatistics. *Environ. Sci. Pollut. Res.* **2017**, *24*, 26350–26374. [[CrossRef](#)]
36. Su, H.; Kang, W.; Xu, Y.; Wang, J. Assessing Groundwater Quality and Health Risks of Nitrogen Pollution in the Shenfu Mining Area of Shaanxi Province, Northwest China. *Expo. Health* **2017**, *10*, 77–97. [[CrossRef](#)]
37. GB/T14848-2017; Standards for Groundwater Quality. Standards Press of China: Beijing, China, 2017.
38. WHO. *Guidelines for Drinking-Water Quality*, 4th ed.; World Health Organ: Geneva, Switzerland, 2011.
39. Carrera-Villacrés, D.; Hidalgo, A.; Guevara-García, P.; Vivero, M.T.; Delgado-Rodríguez, V. Hydrogeochemical analysis of volcanic and geothermal fluids in the Andes from Ecuador using hydrochemical plots (Stiff, Piper and Schoeller-Berkaloff diagrams). *IOP Conf. Ser. Earth Environ. Sci.* **2016**, *39*, 012062. [[CrossRef](#)]
40. Gibbs, R.J. Mechanisms controlling world water chemistry. *Science* **1970**, *170*, 1088–1090. [[CrossRef](#)]
41. Li, X.; Huang, X.; Zhang, Y. Spatio-temporal analysis of groundwater chemistry, quality and potential human health risks in the Pinggu basin of North China Plain: Evidence from high-resolution monitoring dataset of 2015–2017. *Sci. Total Environ.* **2021**, *800*, 149568. [[CrossRef](#)]
42. Rajmohan, N.; Patel, N.; Singh, G.; Amarasinghe, U.A. Hydrochemical evaluation and identification of geochemical processes in the shallow and deep wells in the Ramganga Sub-Basin, India. *Environ. Sci. Pollut. Res. Int.* **2017**, *24*, 21459–21475. [[CrossRef](#)]
43. Nematollahi, M.J.; Ebrahimi, P.; Razmara, M.; Ghasemi, A. Hydrogeochemical investigations and groundwater quality assessment of Torbat-Zaveh plain, Khorasan Razavi, Iran. *Environ. Monit. Assess.* **2015**, *188*, 2. [[CrossRef](#)] [[PubMed](#)]
44. Wu, P.; Tang, C.; Zhu, L.; Liu, C.; Cha, X.; Tao, X. Hydrogeochemical characteristics of surface water and groundwater in the karst basin, southwest China. *Hydrol. Process.* **2009**, *23*, 2012–2022. [[CrossRef](#)]
45. Nakhaei, M.; Dadgar, M.A.; Amiri, V. Geochemical processes analysis and evaluation of groundwater quality in Hamadan Province, Western Iran. *Arab. J. Geosci.* **2016**, *9*, 384. [[CrossRef](#)]
46. Amiri, V.; Nakhaei, M.; Lak, R.; Kholghi, M. Investigating the salinization and freshening processes of coastal groundwater resources in Urmia aquifer, NW Iran. *Environ. Monit. Assess.* **2016**, *188*, 233. [[CrossRef](#)]
47. Yu, Y.; Song, X.; Zhang, Y.; Zheng, F.; Liang, J.; Liu, L. Identifying spatio-temporal variation and controlling factors of chemistry in groundwater and river water recharged by reclaimed water at Huai River, North China. *Stoch. Environ. Res. Risk Assess.* **2013**, *28*, 1135–1145. [[CrossRef](#)]

48. Li, P.; Zhang, Y.; Yang, N.; Jing, L.; Yu, P. Major Ion Chemistry and Quality Assessment of Groundwater in and around a Mountainous Tourist Town of China. *Expo. Health* **2016**, *8*, 239–252. [[CrossRef](#)]
49. Abdesslem, K.; Azedine, H.; Lynda, C. Groundwater hydrochemistry and effects of anthropogenic pollution in Béchar city (SW Algeria). *Desalination Water Treat.* **2015**, *57*, 14034–14043. [[CrossRef](#)]
50. Wu, J.; Li, P.; Qian, H.; Duan, Z.; Zhang, X. Using correlation and multivariate statistical analysis to identify hydrogeochemical processes affecting the major ion chemistry of waters: A case study in Laoheba phosphorite mine in Sichuan, China. *Arab. J. Geosci.* **2013**, *7*, 3973–3982. [[CrossRef](#)]
51. Singh, A.K.; Mondal, G.C.; Singh, T.B.; Singh, S.; Tewary, B.K.; Sinha, A. Hydrogeochemical processes and quality assessment of groundwater in Dumka and Jamtara districts, Jharkhand, India. *Environ. Earth Sci.* **2012**, *67*, 2175–2191. [[CrossRef](#)]
52. Li, P.; Tian, R.; Liu, R. Solute Geochemistry and Multivariate Analysis of Water Quality in the Guohua Phosphorite Mine, Guizhou Province, China. *Expo. Health* **2018**, *11*, 81–94. [[CrossRef](#)]

Disclaimer/Publisher’s Note: The statements, opinions and data contained in all publications are solely those of the individual author(s) and contributor(s) and not of MDPI and/or the editor(s). MDPI and/or the editor(s) disclaim responsibility for any injury to people or property resulting from any ideas, methods, instructions or products referred to in the content.